b

DEVELOPING A METHOD FOR QUANTITATIVE VEGETABLE OIL ANALYSES BY MEANS OF GC-FID

Vi Bui

BACHELOR'S THESIS
November 2020

Energy and Environmental Engineering Degree Programme

ABSTRACT

Tampereen ammattikorkeakoulu
Tampere University of Applied Sciences
Energy and Environmental Engineering Degree Programme

VI BUI:
Developing A Method for Quantitative Vegetable Oil Analyses by Means of GC-FID

Bachelor's thesis 74 pages, appendices 14 pages
December 2020

Vegetable oils in general and specialty oils in specific have an important share in human life not only because their health benefits but also because numerous industrial applications they offer. In order to explore those advantages, the need for oils quantitative analyzing is unquestionable. This paper is a part of finalizing a quantitative approach to analyze vegetable oils by GC-FID. This was done by calibrating standard solution using the already developed GC-FID method. The statistical processing of the calibration results gives parameters that will be used in future analysis of vegetable oils.

There were 16 standards being calibrated in total: squalene; 4 methyl esters: methyl palmitate, methyl linoleate, methyl oleate and methyl stearate; 4 fatty acids: palmitic acid, linoleic acid, oleic acid, stearic acid; α-tocopherol; DL-α-palmitin and a mixture of 5 triacylglycerides: tricaprylin, tricaprin, trilaurin, trimyristin, tripalmitin. By measuring the signals of one or more standard samples with known concentration of analyte, response factors (RF) were calculated. RFs of the methyl esters and squalene are slightly similar, range from 1.13 (methyl oleate) to 1.84 (methyl palmitate). A comparable fashion was found in RFs of the first three triacylglycerides: around 1.5 for tricaprylin, tricaprin and trilaurin. The RFs of other two are 2.66 for trimyristin and 3.14 for tripalmitin. Palmitic acid and DL-a-palmitin share a similar RF, approximately 3.2. A-tocopherol (vitamin E) has a small RF at 1.74. Oleic acid has a slightly bigger RF compare to others, at 3.59. The substances own the highest RFs are stearic acid (4.12) and linoleic acid (5.3). Standards retention times, their limit of detection, limit of quantification and calibration curves were also reported.

The findings will provide a strong foundation for vegetable oil analysis using GC-FID. With the data collected, it is possible to indentify and quantify these chemical substances in future oils investigation.

Key words: GC-FID, quantitative analysis, specialty oils, standard calibration

CONTENTS

ABBREVIATIONS AND TERMS

ASE	Accelerated Solvent Extraction
DAG	Diacylglycerol
FID	Flame Ionization Detector
GC	Gas Chromatography
GC-FID	Gas Chromatography - Flame Ionization Detector
GC-MS	Gas Chromatography - Mass Spectrometry
HPLC	High Performance Liquid Chromatography
ID	Inner diameter
IS	Internal Standard
LOD	Limit of Detection
LOQ	Limit of Quantification
MAG	Monoacylglycerol
MUFA	Monounsaturated Fatty Acids
PUFA	Polyunsaturated Fatty Acids
R^2	Correlation coefficient
RF	Response Factor
Rt	Retention time
SFA	Saturated Fatty Acids
SSL	Split/Splitless
TAG	Triacylglycerol
USFA	Unsaturated Fatty Acids

1 INTRODUCTION

Vegetable fats and oils play an important role in providing essential nutrients for living organisms in the form of food, functional foods, as raw materials for animal feed processing and numerous other essential industries. In order to ensure the quality of input ingredients, detecting the constituents inside the oil is not enough. There is also a demand to understand the quantity of components. Beside contaminants or adulterant, which can greatly decrease oil purity, high amount of free fatty acids in oils also indicates the oil has gone bad since free fatty acids are precursors for peroxides and carbonyl compounds such as aldehydes and ketones, which give a rancid smell to the oil (O'Brien 1998). Development of pharmaceuticals needs quantitative analysis to measure the quality of use materials as well as for monitoring composition of reactions over time (Rome et al. 2012). Moreover, having an insight in the oil composition is also useful to choose proper applications for this material. Therefore, my thesis's objective was focused on developing a quantitative anaylizing method for vegetable oils and fats in general.

This thesis was conducted as a part of my internship at the Centre of Expertise on Sustainable Chemistry of Karel de Grote University of Sciences and Technologies. During my time at the Centre of Expertise, I worked on the ExtReMo project (Specialty Oil: Extraction, Refinement and Modification). ExtReMo aim at consulting the project's clients with several applications for locally produced specialty oils. In this project, a number of 'high-quality oils' will be examined. The different crops are cultivated and processed locally by our test farms partners. The seeds of these crops are extracted and the oils are analyzed to investigate their usefulness in various industrial applications. In order to provide reliable consultation to our customers, an up-to-date analyzing method to study the quantity of oil components is required.

a) Flanders Poppies

(2) Calendula Officinalis (marigold)

(3) Sunflowers

FIGURE 1. Several types of flowers seeds used in ExtReMo (Source: istockphoto.)

When generating a quantitative analyzing method, there are four critical components: sampling, sample preparation, instrument analysis conditions and standardization or calibration (Harris 2007). Fortunately, the first three steps have been well constructed and approved, my role in ExtReMo project was to perform the standard calibration to complete the method developments. Calibration allows the researchers to correlate the FID signal (area counts of the analyte peak) to the actual analyte concentration, therefore being able to quantify them in the long run. However, due to the pandemic, I was not able to finish the work. There were still some other components and finalizing process that need to be worked on.

During my internship, I was able to calibrate 16 oil components in total: squalene; 4 methyl esters include methyl palmitate, methyl linoleate, methyl oleate and methyl stearate; 4 fatty acids which are palmitic acid, linoleic acid, oleic acid, stearic

acid; α-tocopherol;DL-α-palmitin and a mixture of triacylglycerides: tricaprylin, tricaprin, trilaurin, trimyristin, tripalmitin. Their retention times, limit of detection (LOD), limit of quantification (LOQ), average response factors and calibration curves were generated and presented in this report.

2 THEORY

2.1 Specialty Oils

Specialty Oils are vegetable oils, which contain interesting minor components that can be used in industries. Vegetable oils are fats produced from plant-based sources; usually from seeds, nuts, fruits and cereal grains (Hammond 2003). Our generation witnessed a dramatic growth in vegetable oils consumptions. This is the result of many factors including population boom, globalization, agriculture technology, improvements of crop science, oil processing and food manufacturing. Several well-known vegetable oils widely used are soybean, canola, sunflower and peanut. However, with an increasing demand for oils producing, comes several concerns about complex logistic process, rigorous operations and the stability of final products throughout the supply chain, not to mention environmental impacts of oil manufacture and transportation. Moreover, the need for specific fatty components serving different purposes has navigated current productions trends of fats and oils. The industry is leaning towards diversify and discovering new applications for vegetable oils that are locally cultivated and content novel chemical constituents- as known as Specialty oils- by researching naturally bred and modifying the oils to desired formula (Jung et al. 2005). This is also the objective and orientation of ExtReMo project. In order to reach that goal, understanding and having an insight about oils elements is extremely crucial.

2.1.1 Composition

Vegetable oils in general and specialty oils in specific are complicated mixtures contain mostly triacylglycerols (TAGs), which usually accounted for more than 95%. Less than 5% of the substances are diacylglycerols (DAGs) and monoacylglycerols (MAGs). The other 1% are some minor components such as tocopherol, phytosterol, etc. which give the oils their bioactive properties (Hammond 2003).

- **Glycerides**

  - *Triacylglycerols (TAGs)*

The main components of vegetable oils and fats are TAGs (triacylglycerols or triglycerides), which are formed when all three hydroxyl groups of a glycerol molecule undergo an esterification with three fatty acids molecules. (Nelson et al. 2000)

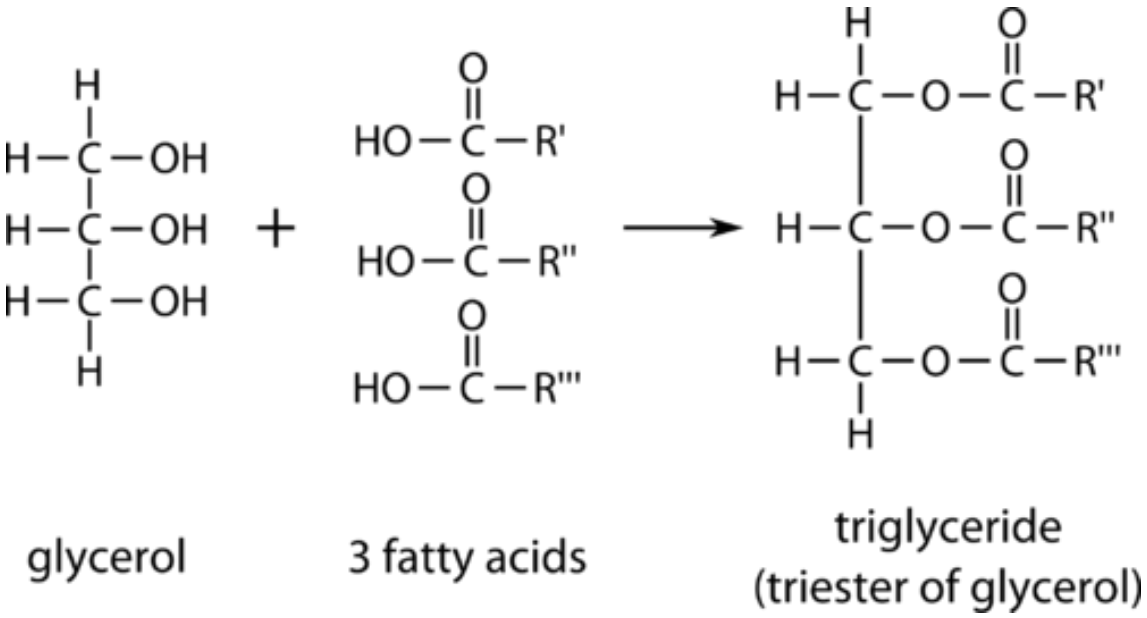

FIGURE 1. TAGs formation (Sheng 2013)

Because of the long carbon chains that TAGs have, oils and fats are nearly nonpolar molecules and easily dissolved in nonpolar organic solvents such as hexane and ethers but not soluble in water, which is a polar solvent (Thomas 2002).

  - *Diacylglycerols (DAGs)*

DAG (diacylglycerol or diglyceride) is a glyceride containing two ester bonds which connects two fatty acids chains with a glycerol. Depending on the position of these linkages, DAGs are divided into 1,2-diacylglycerols and 1,3-diacylglycerols. Normally DAGs are present in many seed oils at a concentration of approximately 1-6% (Flickinger et al. 2003).

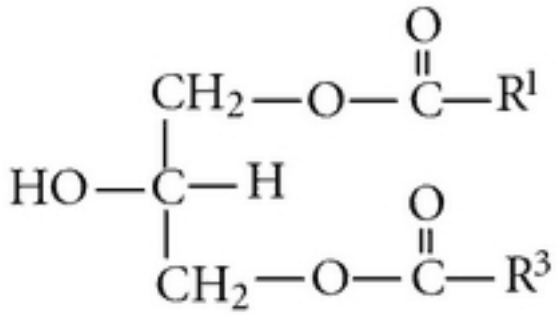

FIGURE 2. Chemical structure of a 1,3-diacylglycerol (Sheng 2013).

- *Monoacylglycerols (MAGs)*

MAGs, also known as monoglyceride, consist of one fatty acid chain covalently bonded to a glycerol molecule through an ester linkage. They are further categorized into 1-monoacylglycerols and 2-monoacylglycerols based on the position of their fatty acids. They are constituents of some seed oils such as olive oil or rapeseed oil but at very insignificant level, around 0.1- 0.2% (Flickinger et al. 2003).

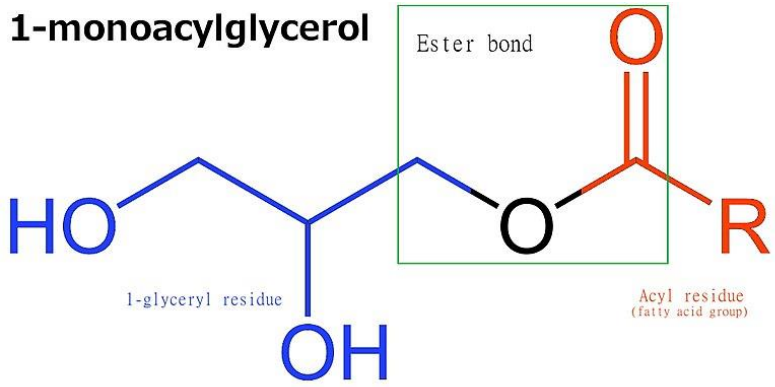

FIGURE 3. Chemical structure of MAG.

Together with DAGs, MAGs are usually applied into food, detergent, plasticizer, cosmetics and pharmaceutical formulations thanks to their emulsifying properties that help prevent separation in mixtures of oils and water (Zheng et al. 2008, Corma et al. 2005). Because their natural occurrence is very low, the primary source for industrial production is biosynthesis from vegetable or animal fat (Sonntag 1982).

- **Fatty Acids**

The fatty acids inside glycerides molecules are key constituents of lipids since they greatly affected oils characteristics. Saturated fat consists of saturated fatty acids (SFA) whose carbon chains are single bonds and saturated with hydrogen atoms. They are mostly found in animal fats and some vegetable oils such as palm oil, coconut oil, etc. Thanks to the single covalent bonds between carbon atoms, their linear molecules can form a dense structure and gain strong inter-molecular interactions. This resulted in a very stable type of fat with high melting points, less prone to oxidative or reacts with other chemicals (Saig 2014). Because of this typical feature, in the past, food processors tended to manufacture these long shelf-life fats. However, some of these oils can cause blockages in blood vessels, coronary arteries and lead to severe cardiovascular disease (Lands 2005; Burr 1994). TABLE 1 bellows introduce several common SFA in vegetable oils.

TABLE 1. Common SFA in vegetable oils (Huber, L. 2007)

IUPAC name	Common name	C:D	Chemical formula	Melting point (℃)	Sources
Dodeca-noic	Lauric	C12:0	$C_{11}H_{23}COOH$	43.2	Coconut, laurel
Tetra-decanoic	Myristic	C14:0	$C_{13}H_{27}COOH$	58	Nutmeg, Palm ker-nel
Hexadec-anoic	Palmitic	C16:0	$C_{15}H_{31}COOH$	62.9	Cotton-seed, soy-bean
Octade-canoic	Stearic	C18:0	$C_{17}H_{35}COOH$	69.6	Shea, Cocoa

Another type of fatty acids is unsaturated fatty acids (USFA). They are found in plant-based fats such as soybeans, peanuts, sesame, flax, almonds, sunflower, cabbage, corn, olives, etc., or in marine animals like whales and salmon, herring, cod, etc. These are fatty acids with one double bond (MUFA - Monounsaturated Fatty Acid) or multiple double bonds (PUFA - Polyunsaturated Fatty Acid) in the structure. In contrast to SFA's linear molecules, USFA can have either *cis* or *trans*

configurations, depending on the relative position of the alkyl groups. In nature most MUFAs have a *cis* configuration (Kenar 2017). The *cis* form causes the hydrocarbon chains to bend, so MUFA in general and USFA in specific does not align as saturated fatty acids, which results in a low melting point and are usually liquid at room temperature. Human body can easily metabolize unsaturated fats thanks to its biochemical active trait (Saig 2014). The C = C double bond position in the USFA carbon chain is a very important factor. If the first pair is three carbons away from the methyl (omega end) of the fatty acid, it is omega 3 fatty acid, denoted by ω-3 or n-3. Similarly, we have omega 6 (ω-6 or n-6), omega 9 (ω-9 or n-9). In foods, α – linolenic acid (ALA, C18: 3n-3) is ω-3 fatty acids, linoleic acid (LA, C18: 2n-6) is ω-6 fatty acid, and oleic acid (18: 1n-9) is the major ω-9 acid. They are USFA with high biological value.

TABLE 2. Common USFA in vegetable oils (Huber, L. 2007)

IUPAC name	**Common name**	**C:D**	**Chemical formula**	**Melting point (℃)**	**Sources**
***cis*–9–Octadecenoic**	Oleic	C18:1n-9	$C_{17}H_{33}COOH$	13	Olive, peanut, sesame
***all–cis*–9,12–Octadecadienoic**	Linoleic (LA)	C18:2n-6	$C_{17}H_{31}COOH$	-5	Sesame, soybean
***all–cis*–9,12,15–Octadecatrienoic**	α–Linolenic (ALA)	C18:3n-3	$C_{17}H_{29}COOH$	-14.5	Flaxseed, rapeseed
***all–cis*–6,9,12–Octadecatrienoic**	γ–Linolenic (GLA)	C18:3n-6	$C_{17}H_{29}COOH$	-14.5	Chia, hempseed

The role of USFA in nutritional health is diverse. The PUFAs have high bioactive properties, good metabolism and positive effects on health such as regulating blood vessel walls, heart protecting, lessening risks of cardiovascular diseases (Bucher et al.2002, Calder 2006, 139]. It is also an anti-cancer agent. A number of studies have reported anti-cancer effects of omega 3 and omega 6 fatty acids, especially breast cancer (Caygill et al. 1995, Deckere 1999, Hibbeln 2006), colon cancer (Caygill et al. 1995, Deckere 1999) and prostate cancer (Augustsson

2003, 131]. In addition, they also reduce the risk of diabetes, asthma, arthritis, improve eyesight, fight depression, avoid stroke, nourish skin, etc. (Illum et al. 1996, Iso et al. 2001, Su et al. 2003)

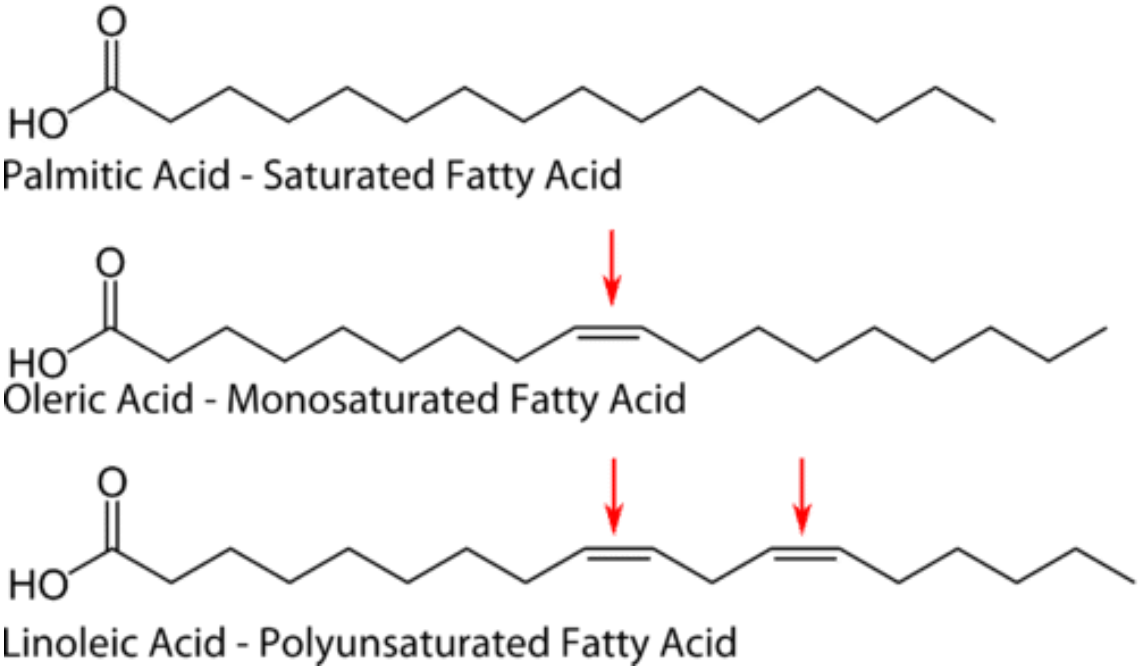

FIGURE 4. Chemical structure of three common fatty acids (Soult 2019)

Naturally, free fatty acid alkyd esters are productions of oils and fats hydrolysis. The presence of free fatty acids in oils might indicates that degradation has occurred through poor handling. Because the oils are exposed to several environments like storage, processing, heating or frying; TAGs are broken down into free fatty acids molecules. Depend on time, temperature and moisture content in the oils, this process can be sped up. Since fatty acids are not stable, they oxidize easily and make the oil turning rancid. Thus, the amount of free fatty acids in oil samples is an indicator for oil quality and overall value. (Yang et al. 2016)

- **Minor Components**

Beside the main components, oils and fat also own numerous minor components that are lipid-soluble, as known as the unsaponifiable materials.

- *Sterols*

Sterols are the major unsaponifiable components: they are cholesterol in animal fats and phytosterols in vegetable oils (Kamal-Eldin, A. 2013). Phytosterols with its health benefits are recommended to increase the daily intake (Bruckert et al. 2011). The most famous and widely demonstrated is that the sterols can lower blood levels of low-density lipoprotein, as a result, also decrease risks of heart disease (Pollak 1953, Kritchevsky et al. 2005, Jones et al. 2009). Several studies also claimed that these oils constituents are linked to reduced risk of cancer (Awad et al. 2000, Woyengo et al. 2009). Phytosterols are easily found in specialty oils: rice bran oil is an outstanding example with approximately 26 mg of total phytosterols in 1 gram of oil (Sugano et al. 1997). Three most common phytosterols are β -sitosterol, campesterol, and stigmasterol (Muti et al. 2003). They are illustrated in FIGURE 5 below along with cholesterol and cycloartenol- a phytosterol synthesis.

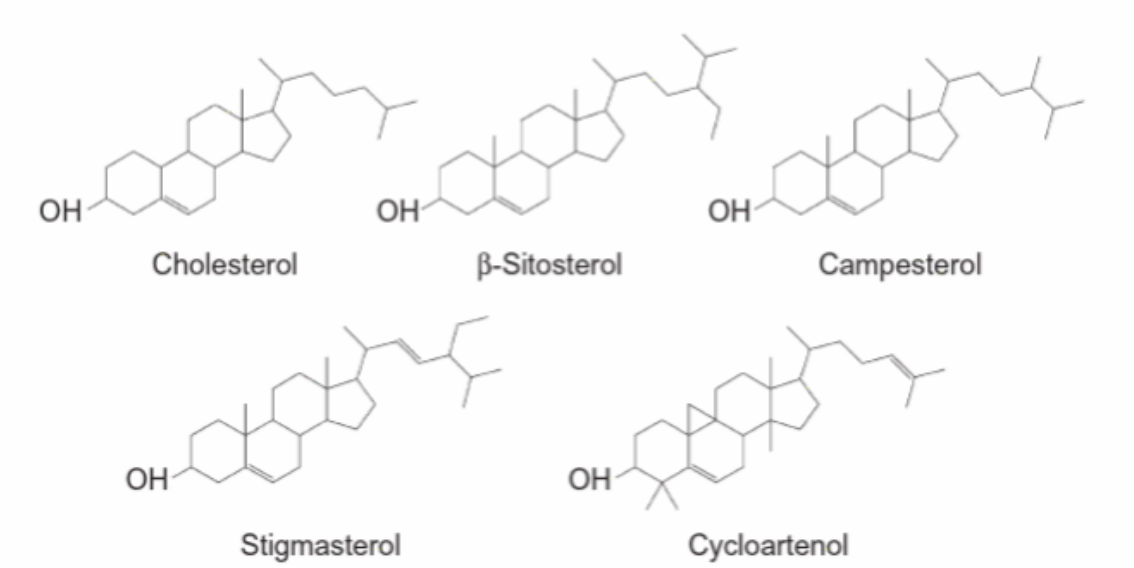

FIGURE 5. Chemical structures of cholestrerol, three phytosterols and cycloartenol (Talbot 2015)

- *Squalene*

A critical precursor of sterols in lipids is squalene. Squalene is a polyunsaturated triterpene consisting of six isoprene units (FIGURE 6). Vitamin D can also be synthesised from squalene (Grimes et al. 1996). Thanks to its ability to prevent oxidative damage induced by UV radiation and being produced by human sebaceous glands, squalene is a popular ingredient in the skin-care industry (Pappas 2009). The substance is believed to inhibiting the formation of cancerous tumors

in the colon, breast, prostate as well as lessening side effects of chemotherapy (Dennis et al. 1989; Ghanbari et al. 2012, Reddy et al. 2009). Another application is squalene-based adjuvants- delivery systems for vaccines. In conjunction with surfactants, it is able to improve vaccine's effectiveness (Reddy et al. 2009). Although this has not been approved by the FDA for use in the United States, this type of adjuvants is currently widely used for influenza vaccines in Europe (Pollack 2009).

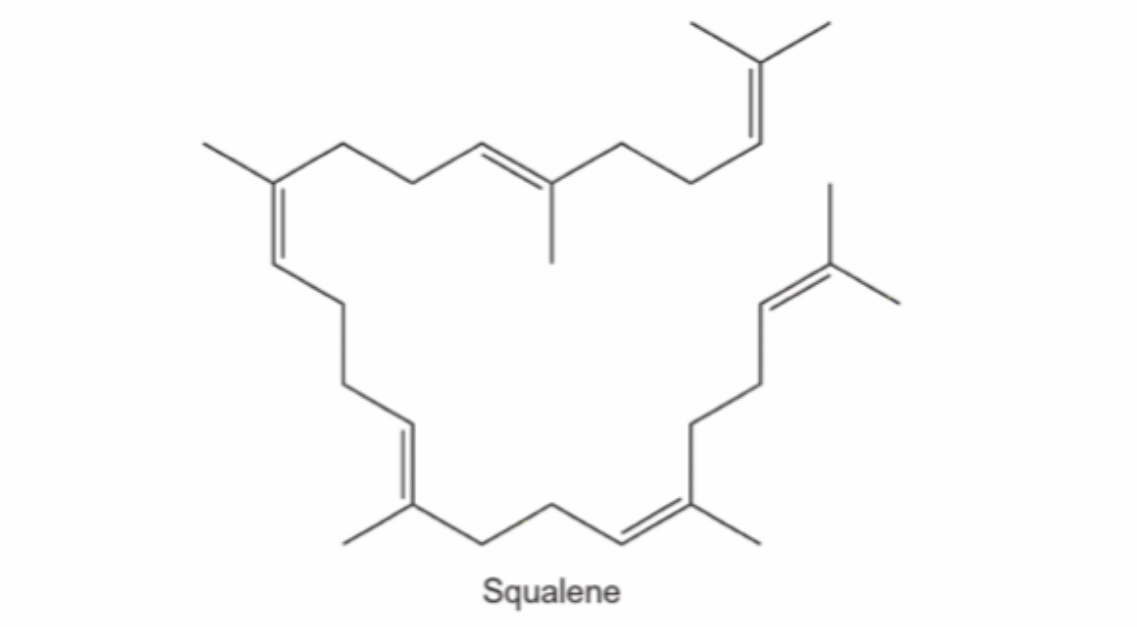

FIGURE 6. Chemical structure of Squalene (Talbot 2015).

Shark's liver is full of squalene in order to keep the animal's body density low (Phleger 1998). Therefore, they are the main sources for conventional squalene extraction. However, environmental and other concerns over shark hunting have motivated its extraction from vegetable sources or biosynthetic processes instead (Wolosik et al. 2013). Two excellent nominees for plant-based squalene are from olive oil and rice bran oil— their constituent contents are ten times greater compare to other plant sources. Rice bran oil has been measured at containing 332 mg/100 g oil, and olive oil are around 100– 700 mg/100 g oil, depending on cultivar and growing conditions (Owen et al. 2000). During ExtReMo project we also found out that amaranth contains a significant amount of squalene.

- *Tocopherols*

Another ubiquitous constituent of vegetable oils that is famous for its oxidative free radical quenching properties is tocopherol (Traber et al. 2007). Tocopherols belong to a category of methylated phenols. They consist of four types of isomers: the α, β, γ, and δ forms. Along with the corresponding unsaturated tocotrienol counterparts, they are known to have Vitamin E activity (Frank 2004, Hensley et al. 2004). Since the 1930s, it has been proved that small quantities of daily consumption of vitamin E (around 15 mg) is necessary for human body function (Fernholz 1938). Tocopherols are also associated with many health benefits, including improvements to macular degeneration and glaucoma, reduce risk of Alzheimer's and Parkinson's disease, prevent tumor formation and limited occurrence of coronary heart disease (Taylor et al. 2002, Morris et al. 2005, Engin et al. 2007, Bhupathiraju et al. 2011). Moreover, vitamin E alone or pair with vitamin C is a famous powerful antioxidants couple that are known to minimize peroxidation at the cellular level and thus help restrain premature cellular aging and tissue degeneration (Kamal-Eldin 2013). Not only attractive to consumers, tocopherols are also valuable for industrial use. Thanks to their capability to improve the shelf life of oils (Choe et al. 2006, Siró et al. 2008), tocopherol can be a type of natural preservative. In the meat industry, there are studies that show the incorporation of tocopherols into animal feed can enhance meat quality and lifespan (Ripoll et al. 2011, Lu et al. 2014).

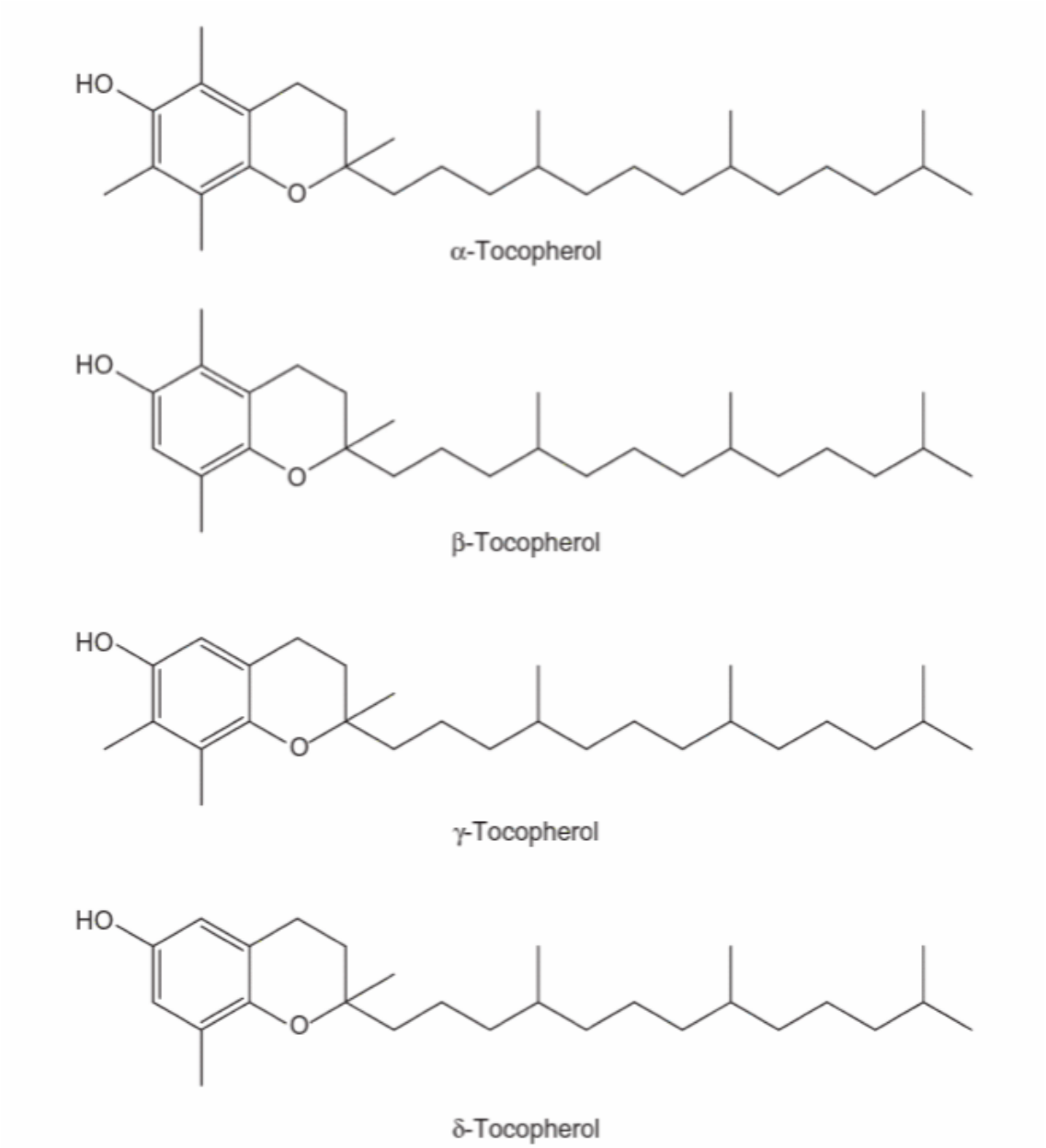

FIGURE 7. Chemical structures of tocopherols (Talbot 2015).

FIGURE 7 above illustrated the structures of four types of tocopherols. The first three types can be found abundantly in algae oil (Frankel et al. 2002). Tree nuts oils such as almonds or hazelnuts are good sources of α -tocopherol (Maguire et al. 2004, Kornsteiner et al. 2006, Ryan et al. 2006). Both β - and γ -tocopherol have notably high quantities inside brazil nuts, pecans, pistachios, primrose and sesame. δ -Tocopherol is harder to find but there are moderate quantities in black currant seed (6.8 mg/100 g oil), borage (5.2 mg/100 g oil), walnut (3.8 mg/100 g oil), shea butter (3.4 mg/100 g oil), and sesame (3.2 mg/100 g oil) (Speek et al. 1985, Reina et al., 1999, Maranz et al. 2004, Eskin 2008).

2.1.2 Extraction

Vegetable oils are usually found in the plant seeds but also occasionally located in other parts such as leaves or fruits. Since different fatty materials have different oil content and properties, there are various extraction methods developed for oil seeds in order to optimize the process by gathering maximum amount of oil from the seeds with minimum costs and time. The four basic categories of vegetable oils extraction are chemical extraction, mechanical extraction, supercritical fluid extraction and steam distillation.

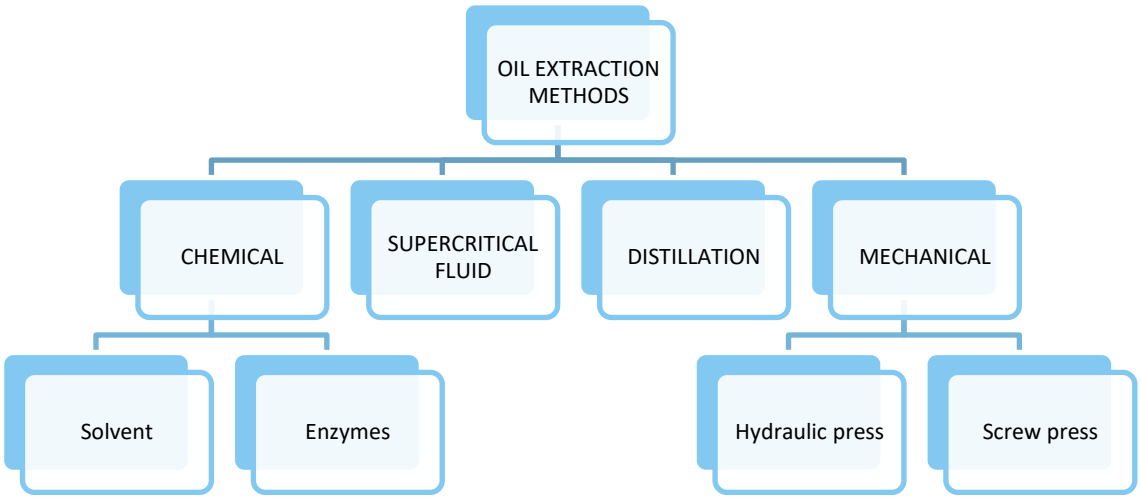

FIGURE 8. Basic methods for vegetable oils extraction (Sari 2006).

The most efficient technique is solvent extraction. It lets a non-polar light paraffinic petroleum fraction, such as pentane, hexane, heptane or octane; come in contact with the seeds and dissolute oil from them (Dunford 2016). In our laboratory, Accelerated Solvent Extraction (ASE) with hexane as solvent was used to extract oil from the sample seeds. ASE, also known as pressurized solvent extraction, is an optimized method from classical methods such as Soxhlet or maceration. Its mechanism is the same but with an addition of increased pressure (100–140 atm) at elevated temperature (50–200 °C). ASE can be performed in both static as well as dynamic mode, or a combination of these two. In static mode, the sample is extracted without any outflow of solvent. When the extraction has reached equilibrium, the sample cell is flushed with solvent and an inert gas to collect the oil. Contrary to that, in dynamic ASE, the extraction solvent is con-

tinuously flowing through the extraction cell. This might resulted in higher extraction yield but also huge demand for solvent, which is not suitable for trace analysis (Mandal et al. 2015). Therefore, static ASE was chosen for our project.

Beside extract our own oil using the ASE, ExtReMo project also received already extracted oil by mechanical pressing from the factory. This is perhaps the oldest and most common method of extracting oil. Through pressing, the seeds are put under the action of compressive external forces and causing the oil to be separate from the oleaginous material called press cake. The de-oiled cake is a high-protein substitute for animal feed (Mariana et al. 2013). FIGURE 9 demonstrates the design of this expeller system. The main advantage of this method is that it allows continuous oil extraction, therefore a large quantity of raw ingredients is handled with minimal labour and cost, not to mention no hazardous substances were release and better oil quality (Dunford 2016). However, usually there will be around 8-14% of oil remain inside the by-product (Bamgboye et al.2007). In fact, our laboratory attempted to re-extract the sample press cakes using ASE and the results showed that oil still took part in approximately 50% of the material. That indicated the current oil expeller system of our supplier is not efficient and need to be upgraded.

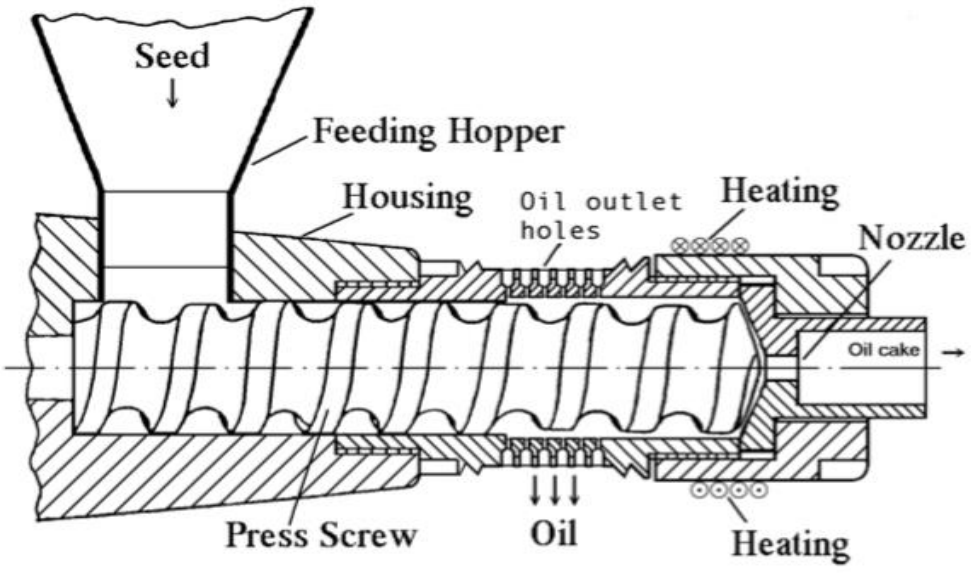

FIGURE 9. Screw press Oil seeds expeller design (Ferchau 2000)

2.1.3 Analysis

Currently, specialty oil analytical studies in the world mainly use chromatographic methods. The comparison andthe selection of chromatographic method used to suit the conditions and purposes of oil analysis is very necessary. Three most common approaches are High Performance Liquid Chromatography (HPLC); Gas Chromatography with Mass Spectrometry (GC-MS) and Gas Chromatography with Flame Ionization Detector (GC-FID).

Due to the low UV absorptivity of many oil components, especially fatty acid, the quantification range of HPLC method is limited. Creating derivatives with chromatophores or luminophores in order to increase detecting sensitivity can solve this problem. Nevertheless, it can result in fronting peak or changing samples properties because of the complicated converting process (IUPAC 1987). In contrast, GC-MS method provides a highly sensitive and stable qualitative analysis based on mass spectrometry. However, the system was not used in our project. It was due to the fact that compounds such as TAGs and DAGs are not very volatile, thus high temperature gas chromatogramphy is needed, using special stainless-steel columns. This cannot be combined with MS. Therefore, in the ExtReMo project, GC- FID was used to analyse and quantify specialty oils.

2.2 Gas Chromatography – Flame Ionization Detector

GC is a commonly used technique in analytical chemistry for separating and examining chemical compounds that stay intact while vaporize. Its two main elements consist of an inert gaseous mobile phase and a liquid stationary phase. Helium or other inactive gas such as nitrogen is usually use as carrier gas in mobile phase (Pavia et al. 2006). In FIGURE 10, several basic GC units are illustrated.

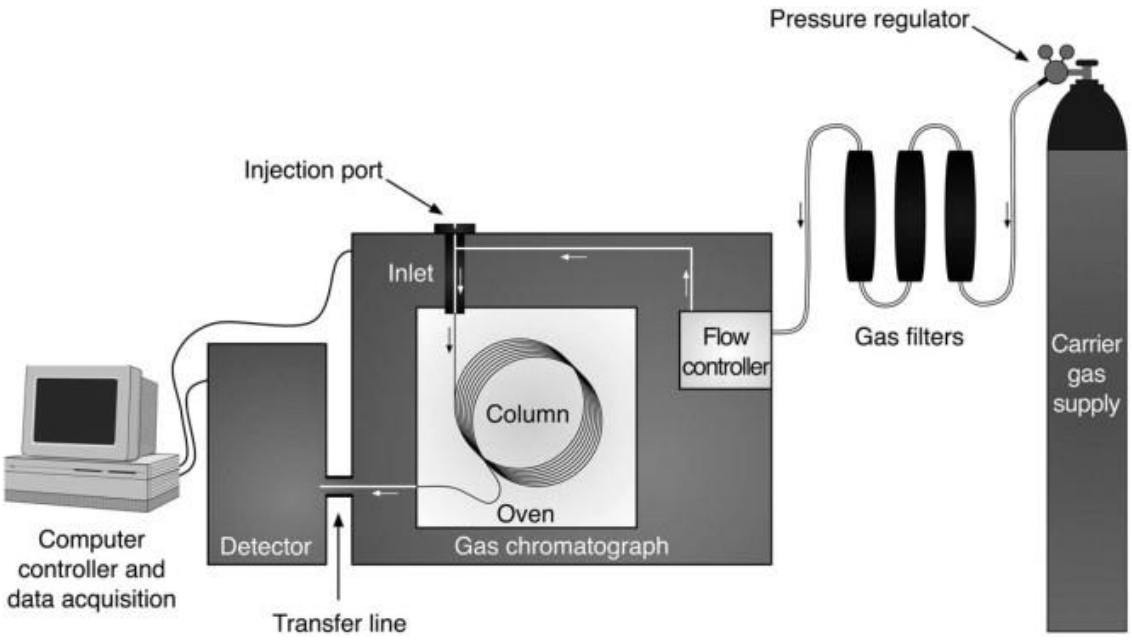

FIGURE 10. A gas chromatography and its main components (Stauffer et al. 2008)

2.2.1 Injector

First, a known volume of sample was introduced into the inlet through an injection port, usually by a micro syringe. In capillary GC, there are four main primary techniques for injection: split, splitless, direct, and on-column injections. Split/splitless (SSL) injectors are the most used. In the split injection mode, only a fraction of the vaporized sample is transferred onto the head of the column. The remainder of the sample is discarded from the injection port via the split vent line. Split injections should be used only when sample concentrations are high enough to allow a portion of the sample to be discarded in order to maintain a sufficient concentration of analytes at the detector to produce a signal. When it comes to low concentration analytes, splitless injection should be operated. In this mode, most of the vaporized sample is transferred to the head of the column (RESTEK 2002).

2.2.2 Column

The mobile phase, which is carrier gas, transfers the evaporated sample from the inlet onto the column, where the stationary phase is. The column is situated in a temperature-controlled oven. When carrier gas with sample sweep through and interact with column wall that is coated with stationary phase, chromatographic separation takes place. Separated components of the sample exit the column and immediately enter a detector in different retention time depend on its properties, which provides an electronic signal proportional to the number of eluting analytes. The comparison of retention times is what gives GC its analytical usefulness (Stauffer et al. 2008).

Choosing the right type of column is crucial for optimizing GC separation and analysis results. The fundamental aspects to be considered when selecting a column are its stationary phase material, inner diameter (ID), film thickness and length. The stationary phase polarity and selectivity are concerns because they will strongly affect the outcome. The material must share the same polarity and selectivity with the analytes to have greater retention. Temperature limit of the material is also crucial. Once the proper stationary phase is selected, column film thickness and inner diameter should be optimized. The thickness (μm) of column film directly affects both sample retention and maximum operating temperature of the column. The thicker the film, the lower the maximum heat. Therefore, extremely volatile compounds are suitable for thick film because they will stay longer in the column, results in more separation. In contrast, high molecular weight compounds are perfect for thin film since their time in the column is shorter and prevent phase bleed at higher elution temperatures. ID does not greatly impact on retention factor like other elements, but it still plays an irreplaceable role in regulating gas flow rate. Due to less mobile phase volume, small ID column (0.15 mm-0.18 mm) generated higher retention factors in shorter analysis time, thus suitable for highly complex samples. The disadvantage is that only split injections are possilble due to the low sample loading capacity. Larger ID (0.25 mm- 0.53 mm) can work with any kind of injection. When it comes to columns length, they are varying from 10 to 105 meters. Longer columns provide better resolution, but they also require more cost and analysis time. Depend on the complexity of the sample, appropriate length should be chosen (RESTEK 2013).

If done correctly, GC method has many advantages such as being able to analyse all fatty acids and its methyl esters of different carbon chain length, degree of unsaturation, position and configuration; high resolution and sensitivity, small sample size, reliable and accurate results (Eder 1995, Shantha et al. 1992). GC is considered to be more economical, effective and analyzing oil components in a shorter time than HPLC method (Quirós et al. 2004).

2.2.3 Detector

In this research, a Flame Ionization Detector (FID) was used to detect specialty oil components. The principle of FID detector is that under the action of a flame at high temperature (hydrogen-air flame) the ionized organic compounds, ions and electrons move to the electrode and form electric current. The current power is then amplified and recorded as a peak. Different components are recorded at different time called retention time (Quirós et al. 2004, Eder 1995).

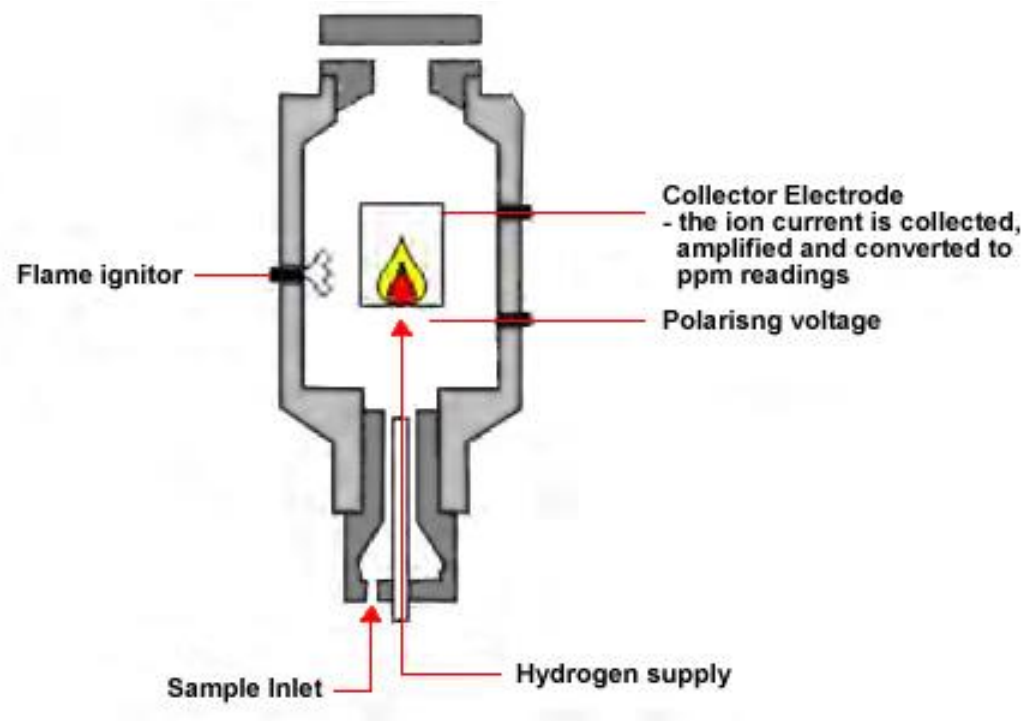

FIGURE 11. A flame ionization detector and its main components (Signal Group)

FID is one of the detectors with good sensitivity, selective with carbon-containing organic compounds, low cost, well known with wide detectable range and high

stability. In fact, Capillary GC-FID is the most widely used technique for quantitative oil analysis (Papazova et al. 1999). However, FID also has the disadvantages of having to use additional gas system. Also the sample components decompose in the flame, so sample cannot be used in the case of allowing the component to go through another analyser (for example infrared device) and when using the FID to analyse new substances, it is impossible to determine without standard calibration (Eder 1995).

2.2.4 Chromatogram

FIGURE 12 below is an example of a type of pumpkin seeds oil's GC-FID chromatogram. It illustrated the signal peaks of each components in the analyte and their retention time. The integration results show the peaks area. From the chromatograms, we can visually compare the signals of different concentrations of a component.

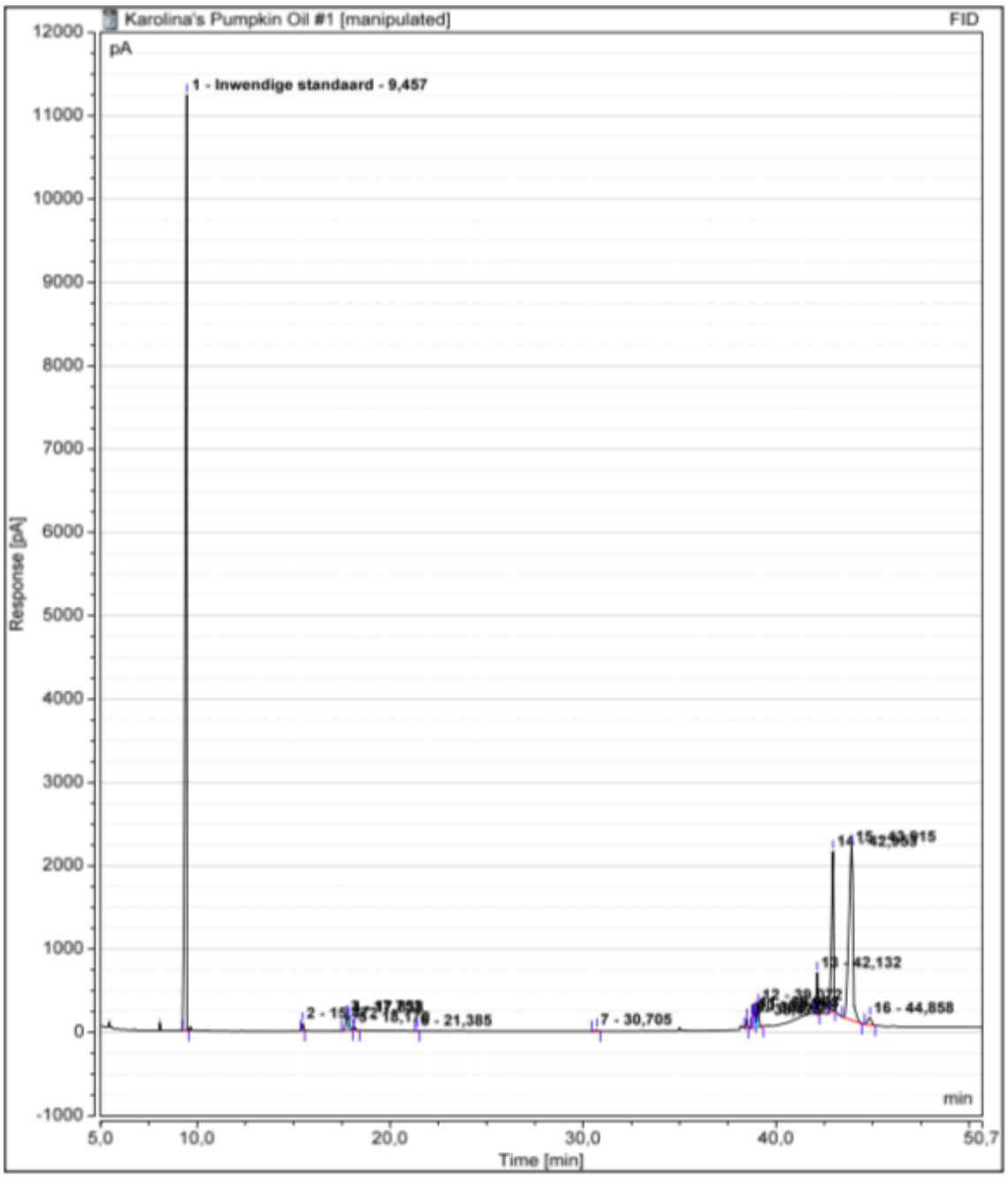

FIGURE 12. KAKAI Pumpkin seeds oil chromatogram (Vi Bui 2020).

2.3 Multiple points internal standard calibration

Calibration is the process of experimentally determining the value of Response Factor between the signal and concentration of an analyte in analytical process. The Response Factors (RF) are the tools to quantify chemical components of this method. Measuring the signals of one or more standard samples with known concentration of analyte makes identification and also quantification possible. When there is more than one standard concentration, a calibration curve can be drawn

from the results by plotting the concentration in the standard sample signal area or height versus the signal area or height. This basic method of calibration is called external standard calibration. However, there is noticeable amount of errors so this technique is only favourable when the examining sample is simple and small or when no instrumental variations are observed (Harvey 2016). In this report, multiple-point internal standard calibration approach was used. It is a more accurate calibration approach and widely used not only in chromatography but also in quantitative HLPC-MS (Burlingame et al. 1998). An Internal Standard (IS) is a substance, different from the analyte, added inside sample solution with known quantity. By adding IS, the method can compensate for both instrumental and sample preparation errors or variations because the ratios between the analytes and IS are constant (Dudley et al. 1978). Tetradecane was chosen as IS for this project because it meets these requirements (Smith et al. 1981):

- Similar in chemical structure and retention with the analyte.
- Not already exist in the sample.
- High purity.
- Good stability.
- Well resolved from the compound of interest.

2.4 LOD & LOQ

Limit of detection (LOD) and limit of quantification (LOQ) are two important performance features in validating a quantitative method. They represent the smallest concentration of an analyte that can be reliably measured by an analytical procedure. The definitions that describe these parameters vary from different guidelines. Likewise, there have been numerous methods for estimating it (Shrivastava, A et al. 2011). According to European Medicines Agency, LOD is defined as the minimum concentration that can be detected but not necessarily quantified. Meanwhile, LOQ is the minimum analyte concentration that can be precisely determined under the stated experimental conditions. In this paper, LOD and LOQ were determined using visual evaluation and calibration curve equation.

3 MATERIAL AND METHODS

3.1 Oil extraction

Extraction of oil from seeds consisted of 5 steps.

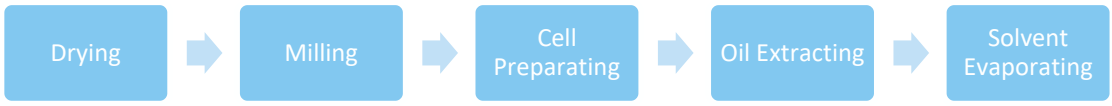

The seeds were first dried and milled in order to increase the contact area and help solvent to penetrate the sample more readily. Milling was performed with the Planetary Mono Mill- Pulverisette 6, which utilizes the centrifugal forces it created from rotating the grinding bowl and the grinding balls inside. By adjusting the speed and running time, it is possible to find settings for highest extraction yield.

The flaked seeds were mixed with Celite with an appropriate proportion before being packed inside a stainless-steel sample cell. Celite, or Diatomaceous earth, is composed of small and hollow particles, which give it high porosity and turn it into an excellent filtration medium. Combining Celite with the milled seeds allows better solvent flow and even more contact surface (Anderson 2004).

The Dionex ASE 350 (FIGURE 13b) was used to extract oil from the flake seeds in static mode. The oven was first heated to 110C, cell loaded into oven, filled with hexane and heated (equilibration). Static extraction lasted for 6 minutes, and after that cell rinsed with fresh solvent and nitrogen used to purge solvent.

The process was repeated three times to ensure that most of the oil was drawn out. The outcome was a mixture of oil and solvent, called miscella, in which hexane was eliminated by a Rotavapor. A Rotavapor is a specialized device to perform a vacuum distillation. It is used to remove relative volatile solvents quickly and easily. The evaporation of the solvent is promoted by applying a reduced pressure, through heat using a water bath and by creating a thin liquid film caused

by the spinning of the round-bottom flask. A cooler is needed for the condensation of the evaporated gas. The final product was weighed then transferred into tightly sealed dark glass bottle and stored in a dry cool place. Exposure to oxygen, light or heat will subject oil to oxidation, eventually turning it rancid.

a) Pulverisette 6

b) Dionex ASE 350

c) Rotavapor

FIGURE 13. Equipment for Oil Extraction (Vi Bui 2020).

3.2 Sample preparation for GC-FID

Since GC-FID is a very accurate method with extremely sensitive detector, analytes must be diluted into a wide range of concentration, from 0.25 ppm up to 2500 ppm. In order to economically get samples with that small amount of standards, dilution procedure is divided into 2 parts: the first one in test tubes and the second one in vials. Internal standard is diluted separately to 100 times and then

added to the vials at the second dilution. This ensures there is always a 1:1000 final dilution of internal standard in the vials.

TABLE 3. Analytes list

No.	Name	Manufacturer
1	Squalene	Sigma-Aldrich
2	Methyl Palmitate	ACROS
3	Methyl Linoleate	ACROS
4	Methyl Oleate	Chem-Lab
5	Methyl Stearate	Chem-Lab
6	Palmitic Acid	Chem-Lab
7	Linoleic Acid	Chem-Lab
8	Oleic Acid	Chem-Lab
9	Stearic Acid	Chem-Lab
10	α-tocopherol	Sigma-Aldrich
11	DL-α-palmitin	Sigma-Aldrich
12	TAGs mixture	Sigma-Aldrich

3.3 GC-FID operation

The device, used for this purpose, is the Thermo Scientific TRACE 1300 with SSL injector, FID detector and a MXT-5 column from Restek®. According to the manufacturer website; MXT-5 column made of Siltek-treated stainless steel (Crossbond diphenyl dimethyl polysiloxane) is suitable to analyze specialty oils' components thanks to its ability to endure high-temperature chromatography and low-polarity phase which shares similar polarity with fatty acids. Its indexes also ensure the best efficiency for oil analysis. PAL System auto-sampler is used to inject samples into the device. The system is controlled with the aid of the Chromeleon 7 software. The processing of the chromatograms is also done with the help of this software.

The order of injections were demonstrated below:

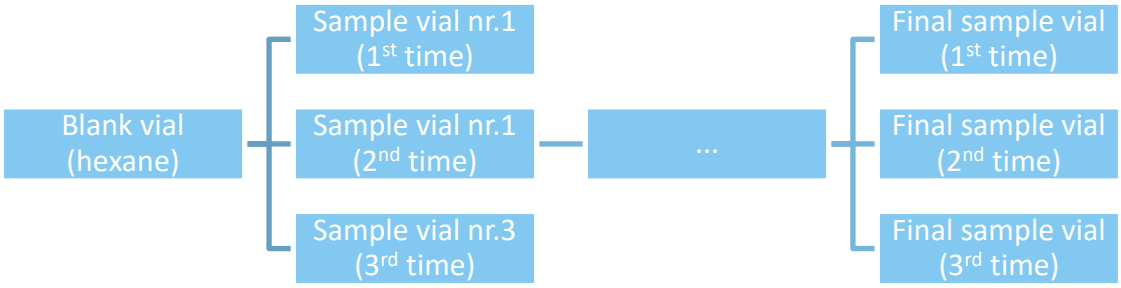

Each vial was injected and analysed three times. Before every sequence, a blank vial, which contains only heptane, was run in order to guarantee the accuracy and to show possible contaminations. The software Chromeleon 7 was used to integrate the chromatograms. These integrations result in a retention time, a peak height and a peak area for each injection. The final reports of the chromatograms were downloaded on to a personal USB for further interpretation.

3.4 Data processing

3.4.1 Calibration curve

The data was transferred and interpreted by Microsoft Excel 2011. Here, the calibration curves of each compound were drawn by plotting the average concentration of substances divided by the concentration of IS (C_{std}/C_{IS}) against the average ratio of peak area of substances divided by the average peak area of IS (S_{Std}/S_{IS}); according to Multiple Point Internal Standard method (Harvey, D. 2016). The equation of the calibration curve is also calculated. In this equation of the curve with formulation y= ax + b, coefficient a is equal to the response factor and coefficient b is the interception with the axis. When its correlation coefficient (R^2) is greater than or equal to 0.99 and the interception is almost 0, the result is within the acceptable range. During the process, abnormal values that can affect the correctness of the graph were eliminated. Determination of the calibration curve is the start of quantitative analysing for a substance in different test sam-

ples. When replacing analyte's area in calibration curve, the corresponding concentration can be calculated. The curve equations are also used in figuring out Limit of Quantification.

3.4.2 Response Factor

Response Factors (RF) of each concentration were calculated using the formula below (Harris, D.2007):

$$RF = \frac{C_{Std}}{S_{Std}} \times \frac{S_{IS}}{C_{IS}} \quad (1)$$

Where:

RF: Response Factor

S_{Std} : Area of analyte signal

C_{Std} : Concentration of analyte

S_{IS} : Area of internal standard signal

C_{IS} : Concentration of internal standard

The average Response Factor of every concentration will be the Response Factor of the Standard.

3.4.3 LOD & LOQ

In general, the LOD of an analytical procedure is the lowest amount of analyte present in the test sample that is detectable and does not need to be accurately determined (European Medicines Agency, 2011). Direct technique was used to detect the value: successively decreased the concentrations of prepared standards until the smallest visible peak. If there is a clear peak of the component in chromatogram, that concentration is still in detection limit.

Meanwhile, LOQ is the lowest amount of analyte in the sample that can be quantitatively calculated with suitable precision under the stated conditions of test (European Medicines Agency, 2011). It was estimated by comparing the theoretical

corrected concentrations (C_{std}/C_{IS}), which are the value of y when substitute corrected area (S_{Std}/S_{IS}) with x in equivalent calibration curve equations; to the reality corrected concentrations in the sample. ExtReMo project accepted a 70% accuracy, therefore, if the relative differences are under 30%, the concentrations are within quantitation limit.

The formula below was used to calculate the relative differences:

$$Relative\ difference = \frac{|y - Reality\ Concentration\ factor|}{y} \times 100\% \qquad (2)$$

4 RESULTS

4.1 Squalene

According to the analysis, squalene has:

- Average Rt: 30.3 minutes.
- LOD ≤ 2.5 ppm.
- LOQ: 50 ppm.
- Average RF: 1.1439

Following concentrations of squalene were being analysed: 2.5 ppm, 5 ppm, 10 ppm, 25 ppm, 50 ppm, 100 ppm, 250 ppm, 500 ppm, 1000 ppm, 2500 ppm. Based on the chromatograms that GC-FID generated, the signals remained in symmetrical shape from 2.5 ppm to 50 ppm. From 100 ppm the peaks started to show fronting.

A 10 points calibration curve with its equation and R^2 was constructed using given results.

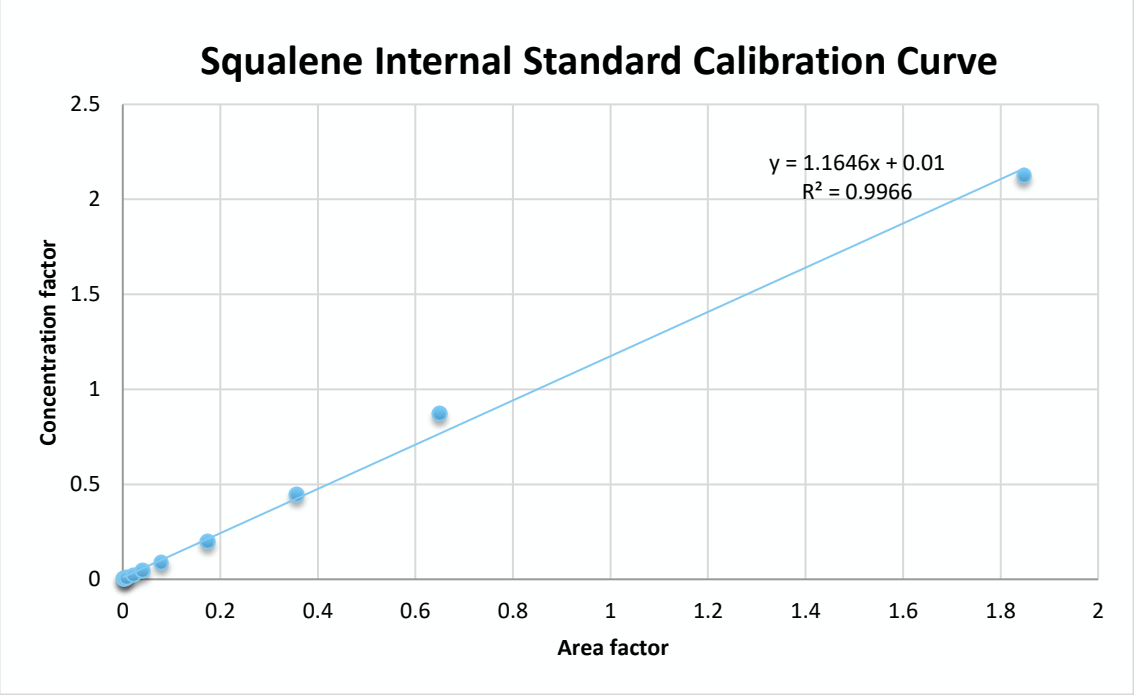

FIGURE 14. Squalene Calibration Curve.

The table below reveal an overall peak area factor, theoretical and reality concentration factor plus their relative differences together with average Rt at each concentration.

TABLE 4. Squalene overall results.

ppm	Corrected area factor	Reality concentration factor	Theoretical concentration factor (y)	Relative difference (%)	Average Rt (minutes)
2.5	0.0017	0.0021	0.0120	82.82	30.26
5	0.0040	0.0042	0.0146	71.60	30.23
10	0.0075	0.0081	0.0187	56.90	30.21
25	0.0222	0.0232	0.0358	35.39	30.22
50	0.0407	0.0439	0.0574	23.49	30.24
100	0.0793	0.0881	0.1023	13.94	30.25
250	0.1735	0.1978	0.2121	6.76	30.28
500	0.3571	0.4444	0.4259	4.34	30.36
1000	0.6496	0.8718	0.7665	13.73	30.30
2500	1.8483	2.1245	2.1625	1.76	30.63

TABLE 4 shows that average Rt increased from 30.21 minutes to 30.63 minutes along with concentration. At 50 ppm, the relative difference between theoretical concentration factor and the reality one is 23.49%, smaller than 30%, therefore 50 ppm is the component LOQ.

4.2 Methyl Palmitate

The results show that methyl palmitate has:

- Average Rt: 15.03 minutes.
- LOD ≤ 0.5 ppm.
- LOQ: 2.5 ppm.
- Average Response Factor: 1.8380

Following concentrations of methyl palmitate were being analysed: 0.5 ppm, 1 ppm, 2.5 ppm, 5 ppm, 10 ppm, 25 ppm, 50 ppm, 100 ppm, 250 ppm, 500 ppm, 1000 ppm. Based on the chromatograms that GC-FID generated, the signals remained in symmetrical shape from 0.5 ppm until 100 ppm. From 250 ppm the peaks started to show fronting.

A 11 points calibration curve with its equation and R^2 was constructed using given results.

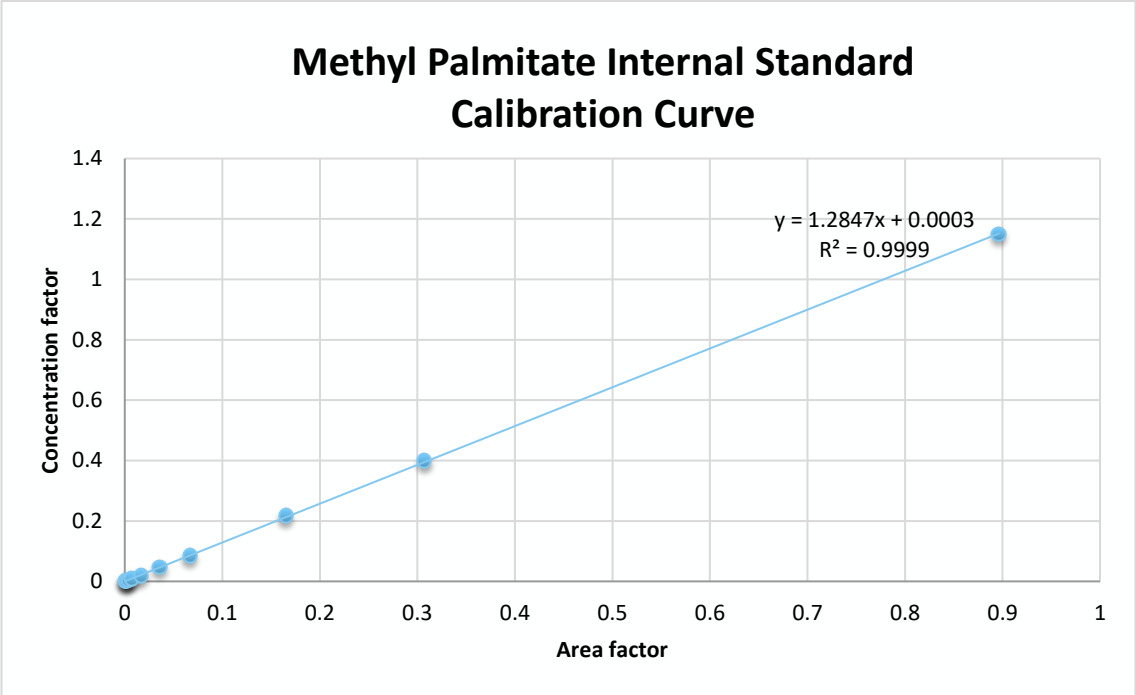

FIGURE 15. Methyl Palmitate Calibration Curve.

The table below reveal an overall peak area factor, theoretical and reality concentration factor plus their relative differences together with average Rt at each concentration.

TABLE 5. Methyl Palmitate overall results.

ppm	Corrected area factor	Reality concentration factor	Theoretical concentration factor (y)	Relative difference (%)	Average Rt (minutes)
0.5	0.0005	0.0005	0.0009	50.96	14.98
1	0.0013	0.0014	0.0020	30.09	14.99

2.5	0.0017	0.0021	0.0025	15.11	15.01
5	0.0041	0.0039	0.0055	28.41	15.01
10	0.0072	0.0089	0.0095	6.91	15.01
25	0.0167	0.0199	0.0218	8.57	15.01
50	0.0360	0.0466	0.0465	0.18	15.01
100	0.0669	0.0838	0.0862	2.84	15.02
250	0.1653	0.2179	0.2127	2.46	15.06
500	0.3073	0.4002	0.3950	1.32	15.08
1000	0.8962	1.1492	1.1517	0.22	15.16

TABLE 5 shows that average Rt increased from 14.98 minutes to 15.16 minutes along with concentration. At 2.5 ppm, the relative difference between theoretical concentration factor and the reality one is 15.11%, smaller than 30%, therefore 2.5 ppm is the component LOQ.

4.3 Methyl Linoleate

After the analysis, these data of methyl linoleate was collected:

- Average Rt: 17.04 minutes.
- LOD ≤ 0.5 ppm.
- LOQ: 10 ppm.
- Average Response Factor: 1.1588

Following concentrations of methyl linoleate were being analysed: 0.5 ppm, 1 ppm, 2.5 ppm, 5 ppm, 10 ppm, 25 ppm, 50 ppm, 100 ppm, 250 ppm, 500 ppm, 1000 ppm. Based on the chromatograms that GC-FID generated, the signals remained in symmetrical shape from 0.5 ppm until 100 ppm. From 250 ppm the peaks started to show fronting.

A 11 points calibration curve with its equation and R^2 was constructed using given results.

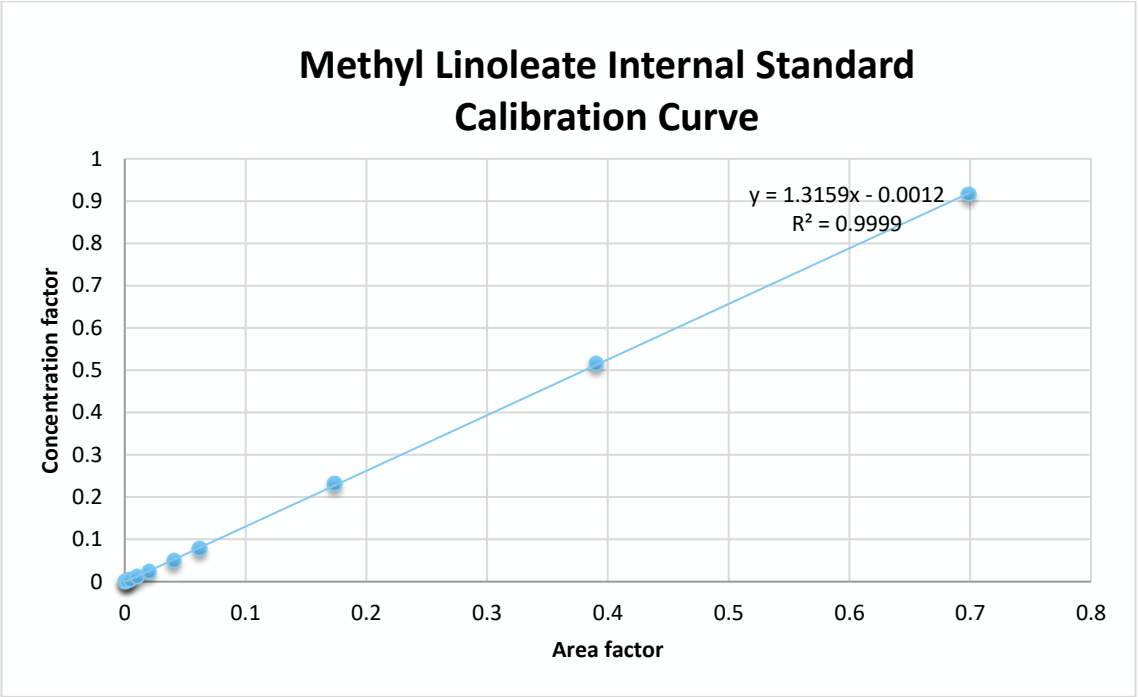

FIGURE 16. Methyl Linoleate Calibration Curve.

The table below reveal an overall peak area factor, theoretical and reality concentration factor plus their relative differences together with average Rt at each concentration.

TABLE 6. Methyl Linoleate overall results.

ppm	Corrected area factor	Reality concentration factor	Theoretical concentration factor (y)	Relative difference (%)	Average Rt (minute)
0.5	0.0005	0.0005	0.0018	72.98	17.02
1	0.0011	0.0010	0.0025	60.61	17.01
2.5	0.0021	0.0024	0.0039	37.03	17.01
5	0.0045	0.0045	0.0071	35.51	17.01
10	0.0104	0.0120	0.0148	18.64	17.01
25	0.0200	0.0230	0.0274	16.00	17.01
50	0.0407	0.0496	0.0546	9.15	17.02
100	0.0620	0.0777	0.0827	6.13	17.03
250	0.1738	0.2323	0.2298	1.11	17.07

500	0.3904	0.5160	0.5148	0.23	17.12
1000	0.6989	0.9159	0.9208	0.54	17.18

TABLE 6 shows that average Rt increased from 17.01 minutes to 17.18 minutes along with concentration. At 10 ppm, the relative difference between theoretical concentration factor and the reality one is 18.64%, smaller than 30%, therefore 10 ppm is the component LOQ.

4.4 Methyl Oleate

The final results of Methyl Oleate are:

- Average Rt: 17.08 minutes.
- LOD ≤ 0.5 ppm.
- LOQ: 25 ppm.
- Average Response Factor: 1.1366

Following concentrations of methyl oleate were being analysed: 0.25 ppm, 0.5 ppm, 1 ppm, 2.5 ppm, 5 ppm, 10 ppm, 25 ppm, 50 ppm, 100 ppm, 250 ppm, 500 ppm, 1000 ppm. From the chromatograms that GC-FID generated, all the peaks were split, from 250 ppm the peaks started to show fronting.

A 12-point calibration curve with its equation and R^2 was constructed using given results.

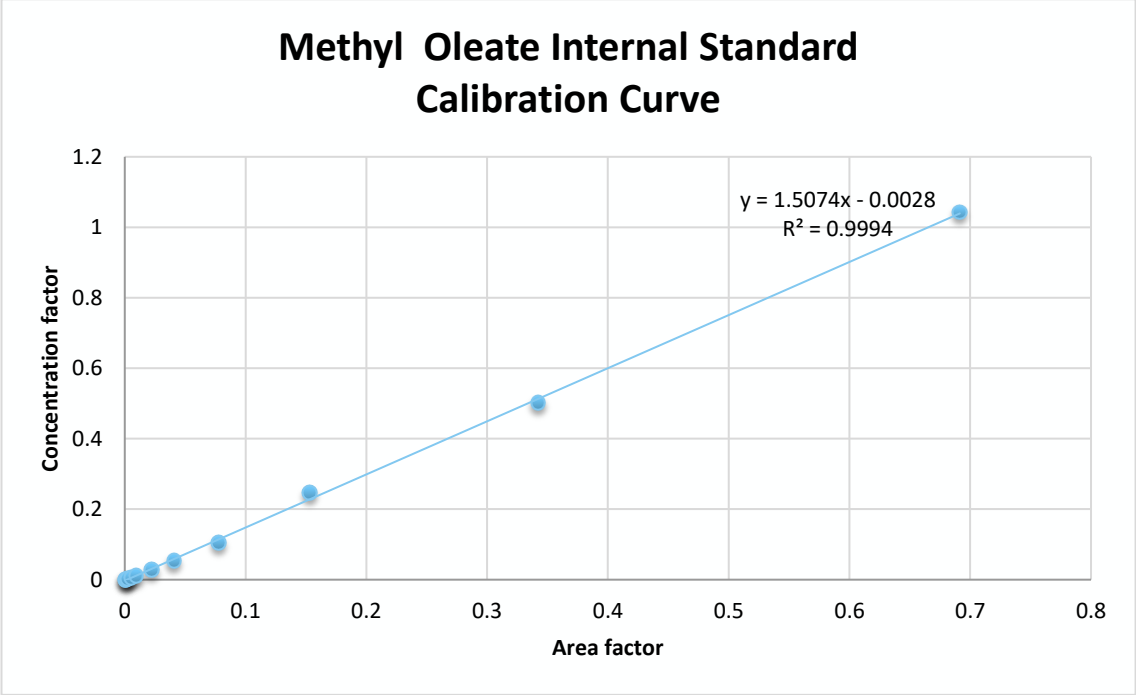

FIGURE 17. Methyl Oleate Calibration Curve.

The table below reveal an overall peak area factor, theoretical and reality concentration factor plus their relative differences together with average Rt at each concentration.

TABLE 7. Methyl Oleate overall results.

ppm	Corrected area factor	Reality concentration factor	Theoretical concentration factor (y)	Relative difference (%)	Average Rt (minutes)
0.5	0.0007	0.0005	0.0039	87.51	17.05
1	0.0013	0.0011	0.0048	77.92	17.04
2.5	0.0027	0.0026	0.0068	61.17	17.04
5	0.0053	0.0057	0.0108	47.20	17.04
10	0.0094	0.0112	0.0170	33.90	17.05
25	0.0224	0.0280	0.0366	23.59	17.05
50	0.0407	0.0528	0.0642	17.69	17.06
100	0.0778	0.1039	0.1200	13.44	17.08
250	0.1532	0.2470	0.2337	5.69	17.08

500	0.3423	0.5021	0.5189	3.23	17.15
1000	0.6914	1.0423	1.0450	0.26	17.19

TABLE 7 shows that average Rt increased from 17.04 minutes to 17.19 minutes along with concentration. At 25 ppm, the relative difference between theoretical concentration factor and the reality one is 23.59%, smaller than 30%, therefore 25 ppm is the component LOQ.

4.5 Methyl Stearate

The results show that methyl stearate has:

- Average Rt: 17.52 minutes.
- LOD ≤ 0.25 ppm.
- LOQ: 10 ppm.
- Average Response Factor: 1.2875

Following concentrations of methyl stearate were being analysed: 0.25 ppm, 0.5 ppm, 1 ppm, 2.5 ppm, 5 ppm, 10 ppm, 25 ppm, 50 ppm, 100 ppm, 250 ppm, 500 ppm, 1000 ppm. Based the chromatograms that GC-FID generated, the signals remained in symmetrical shape from 0.25 ppm until 100 ppm. From 250 ppm the peaks started to show fronting.

A 12 points calibration curve with its equation and R^2 was constructed using given results.

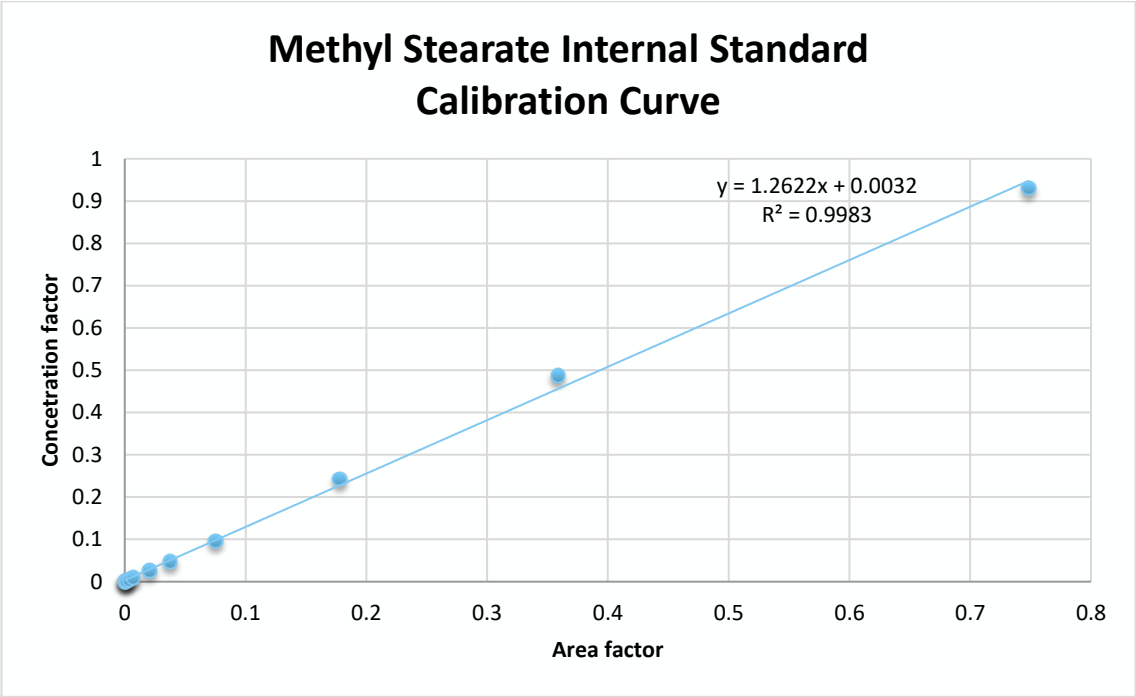

FIGURE 18. Methyl Stearate Calibration Curve.

The table below reveal an overall peak area factor, theoretical and reality concentration factor plus their relative differences together with average Rt at each concentration.

TABLE 8. Methyl Stearate overall results.

ppm	Corrected area factor	Reality concentration factor	Theoretical concentration factor (y)	Relative difference (%)	Average Rt (minutes)
0.25	0.0003	0.0003	0.0035	91.50	17.60
0.5	0.0004	0.0005	0.0037	85.28	17.54
1	0.0007	0.0010	0.0041	76.19	17.47
2.5	0.0018	0.0023	0.0055	58.77	17.46
5	0.0037	0.0046	0.0078	41.08	17.46
10	0.0070	0.0095	0.0120	20.61	17.46
25	0.0207	0.0252	0.0293	14.12	17.47
50	0.0375	0.0476	0.0505	5.76	17.48
100	0.0751	0.0961	0.0980	1.97	17.49

250	0.1777	0.2422	0.2275	6.43	17.54
500	0.3587	0.4865	0.4560	6.71	17.59
1000	0.7483	0.9301	0.9477	1.85	17.68

TABLE 8 shows that average Rt increased from 17.46 minutes to 17.68 minutes along with concentration. At 10 ppm, the relative difference between theoretical concentration factor and the reality one is 20.61%, smaller than 30%, therefore 10 ppm is the component LOQ.

4.6 Palmitic Acid

According to the analysis, palmitic acid has:

- Average Rt: 15.42 minutes.
- LOD ≤ 2.5 ppm.
- LOQ: 10 ppm.
- Average Response Factor: 3.2849

Following concentrations of palmitic acid were being analysed: 2.5 ppm, 5 ppm, 10 ppm, 25 ppm, 50 ppm, 100 ppm, 250 ppm, 500 ppm, 1000 ppm. Based on the chromatograms that GC-FID generated, the signals remained in symmetrical shape from 2.5 ppm until 50 ppm. From 100 ppm the peaks started to show fronting. At 1000 ppm, the peaks were not correct anymore.

A 8 points calibration curve with its equation and R^2 was constructed using given results.

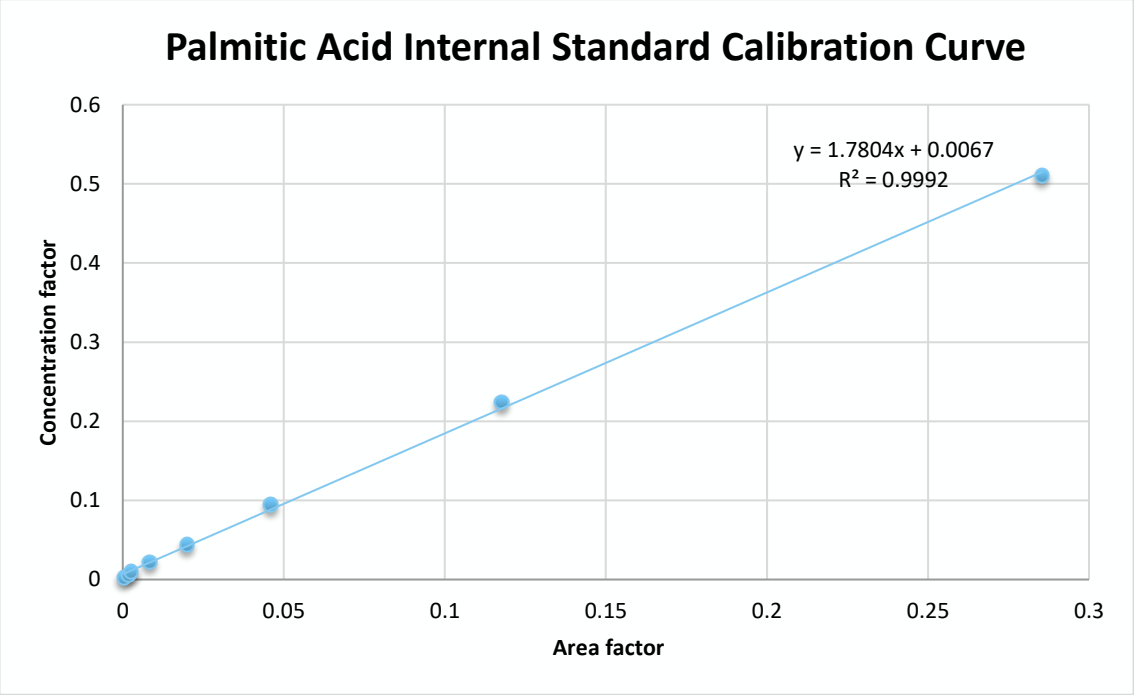

FIGURE 19. Palmitic Acid Calibration Curve.

The table below reveal an overall peak area factor, theoretical and reality concentration factor plus their relative differences together with average Rt at each concentration.

TABLE 9. Palmitic Acid overall results.

ppm	Corrected area factor	Reality concentration factor	Theoretical concentration factor (y)	Relative difference (%)	Average Rt (minutes)
2.5	0.0004	0.0021	0.0075	71.22	15.33
5	0.0018	0.0055	0.0100	45.20	15.33
10	0.0026	0.0099	0.0114	12.66	15.32
25	0.0085	0.0218	0.0217	0.26	15.35
50	0.0200	0.0440	0.0423	4.02	15.39
100	0.0459	0.0942	0.0884	6.58	15.43
250	0.1176	0.2239	0.2161	3.62	15.55
500	0.2854	0.5106	0.5148	0.83	15.67

TABLE 9 shows that average Rt increased from 15.32 minutes to 15.67 minutes along with concentration. At 10 ppm, the relative difference between theoretical concentration factor and the reality one is 12.66%, smaller than 30%, therefore 10 ppm is the component LOQ.

4.7 Linoleic Acid

The results show that linoleic acid has:

- Average Rt: 17.62 minutes.
- LOD: 2.5 ppm.
- LOQ: 10 ppm.
- Average Response Factor: 5.2979

Following concentrations of linoleic acid were being analysed: 1 ppm, 2.5 ppm, 5 ppm, 10 ppm, 25 ppm, 50 ppm, 100 ppm, 250 ppm, 500 ppm, 1000 ppm. There was no peak detected at 1 ppm. Based on the chromatograms that GC-FID generated, first three concentration resulted in tailing peaks, the signals remained in symmetrical shape from 25 ppm until 100 ppm, the peaks became fronting starting at 250 ppm. At 1000 ppm, the peaks were not correct anymore.

A 8 points calibration curve with its equation and R^2 was constructed using given results.

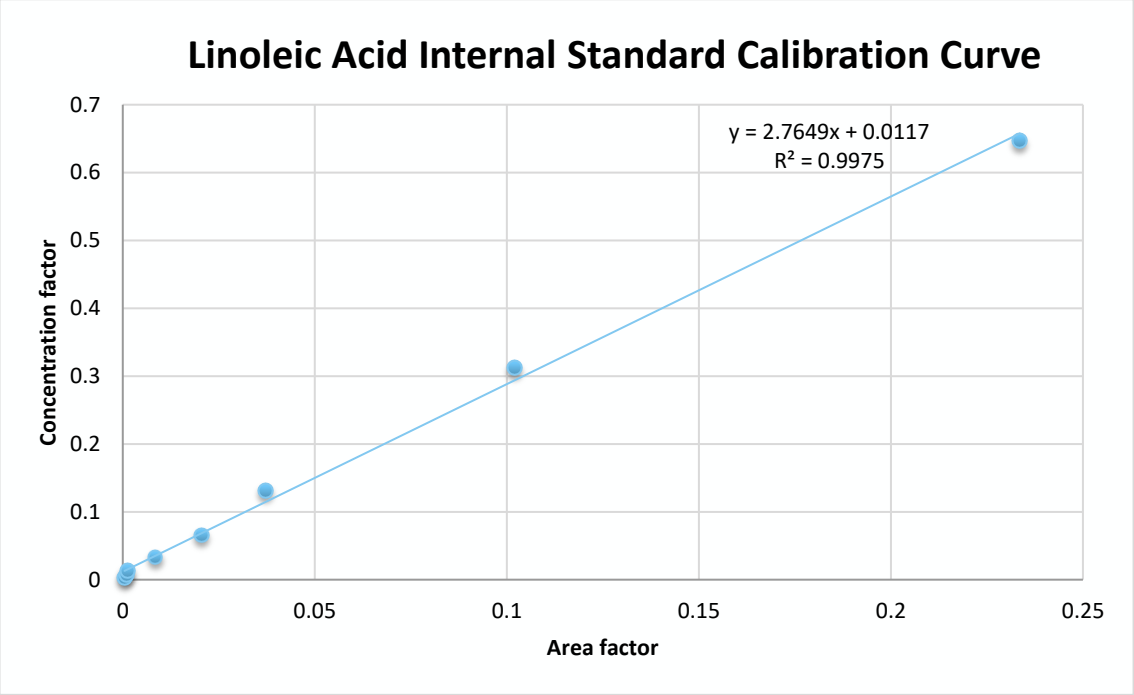

FIGURE 20. Linoleic Acid Calibration Curve.

The table below reveal an overall peak area factor, theoretical and reality concentration factor plus their relative differences together with average Rt at each concentration.

TABLE 10. Linoleic Acid overall results.

ppm	Corrected area factor	Reality concentration factor	Theoretical concentration factor (y)	Relative difference (%)	Average Rt (minutes)
2.5	0.0005	0.0026	0.0130	80.02	17.56
5	0.0009	0.0070	0.0143	51.35	17.55
10	0.0012	0.0129	0.0150	14.22	17.52
25	0.0085	0.0334	0.0351	4.84	17.54
50	0.0205	0.0653	0.0683	4.34	17.58
100	0.0372	0.1313	0.1147	14.53	17.63
250	0.1021	0.3123	0.2940	6.22	17.74
500	0.2336	0.6473	0.6575	1.56	17.89

TABLE 10 shows that average Rt increased from 17.52 minutes to 17.89 minutes along with concentration. At 10 ppm, the relative difference between theoretical concentration factor and the reality one is 14.22%, smaller than 30%, therefore 10 ppm is the component LOQ.

4.8 Oleic Acid

According to the analysis, oleic acid has:

- Average Rt: 17.70 minutes.
- LOD ≤ 2.5 ppm.
- LOQ: 10 ppm.
- Average Response Factor: 3.5855

Following concentrations of oleic acid were being analysed: 2.5 ppm, 5 ppm, 10 ppm, 25 ppm, 50 ppm, 100 ppm, 250 ppm, 500 ppm, 1000 ppm. Based on the chromatograms that GC-FID generated, first three concentration resulted in tailing peaks, the signals remained in symmetrical shape from 10 ppm until 100 ppm, the peaks became fronting starting at 250 ppm.

A 9 points calibration curve with its equation and R^2 was constructed using given results.

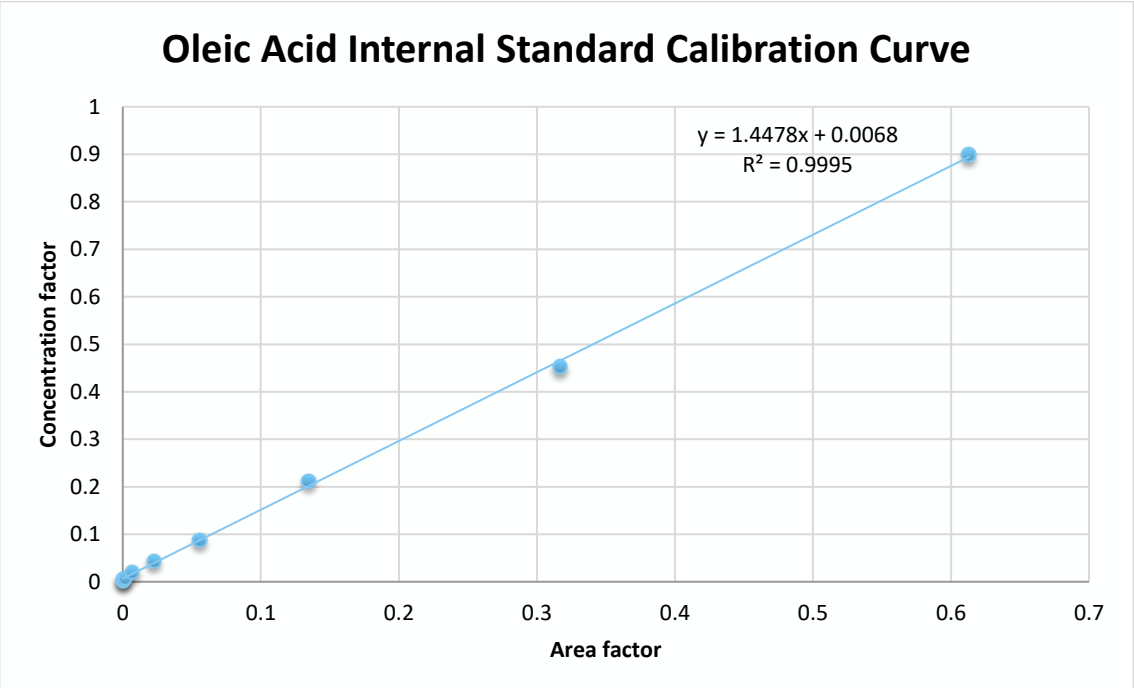

FIGURE 21. Oleic Acid Calibration Curve.

The table below reveal an overall peak area factor, theoretical and reality concentration factor plus their relative differences together with average Rt at each concentration.

TABLE 11. Oleic Acid overall results.

ppm	Corrected area factor	Reality concentration factor	Theoretical concentration factor (y)	Relative difference (%)	Average Rt (minutes)
2.5	0.0002	0.0023	0.0072	67.82	17.56
5	0.0007	0.0047	0.0079	39.92	17.55
10	0.0017	0.0079	0.0093	15.48	17.55
25	0.0068	0.0204	0.0167	22.36	17.56
50	0.0227	0.0436	0.0397	9.74	17.60
100	0.0557	0.0879	0.0874	0.55	17.66
250	0.1347	0.2118	0.2018	4.98	17.77
500	0.3169	0.4522	0.4656	2.87	17.93
1000	0.6128	0.8985	0.8940	0.50	18.11

TABLE 11 shows that average Rt increased from 17.55 minutes to 18.11 minutes along with concentration. At 10 ppm, the relative difference between theoretical concentration factor and the reality one is 15.48%, smaller than 30%, therefore 10 ppm is the component LOQ.

4.9 Stearic Acid

The results of stearic acid are:

- Average Rt: 18.08 minutes.
- LOD: 5 ppm.
- LOQ: 25 ppm.
- Average Response Factor: 4.1173

Following concentrations of stearic acid were being analysed: 2.5 ppm, 5 ppm, 10 ppm, 25 ppm, 50 ppm, 100 ppm, 250 ppm, 500 ppm, 1000 ppm. From the chromatograms that GC-FID generated, there was no peak at 2.5 ppm, the other signals remained in symmetrical shape from 5 ppm until 100 ppm. From 250 ppm the peaks started to show fronting. Moreover, there were some split peaks between 10 ppm and 50 ppm.

An 8 points calibration curve with its equation and R^2 was constructed using given results.

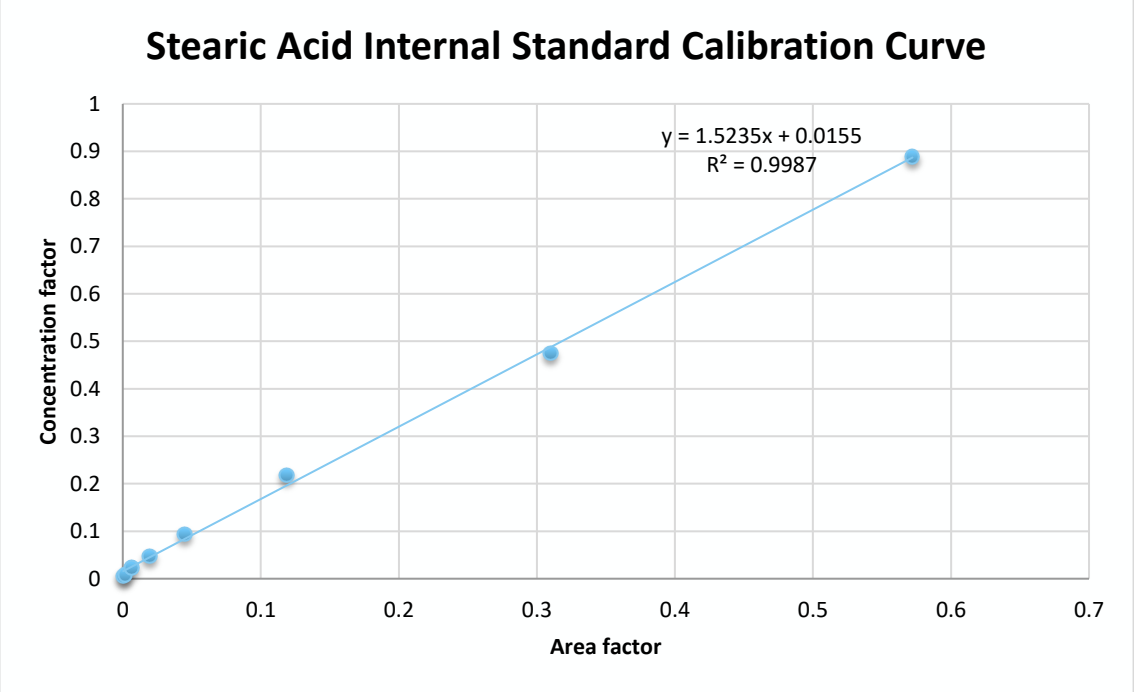

FIGURE 22. Stearic Acid Calibration Curve.

The table below reveal an overall peak area factor, theoretical and reality concentration factor plus their relative differences together with average Rt at each concentration.

TABLE 12. Stearic Acid overall results.

ppm	Corrected area factor	Reality concentration factor	Theoretical concentration factor (y)	Relative difference (%)	Average Rt (minutes)

5	0.0003	0.0048	0.0160	69.81	17.91
10	0.0019	0.0090	0.0184	51.38	17.91
25	0.0064	0.0233	0.0253	7.87	17.92
50	0.0194	0.0475	0.0451	5.34	17.95
100	0.0447	0.0934	0.0837	11.60	18.02
250	0.1189	0.2177	0.1966	10.75	18.14
500	0.3100	0.4754	0.4877	2.53	18.31
1000	0.5721	0.8885	0.8871	0.16	18.46

TABLE 12 shows that average Rt increased from 17.91 minutes to 18.46 minutes along with concentration. At 25 ppm, the relative difference between theoretical concentration factor and the reality one is 7.87%, smaller than 30%, therefore 25 ppm is the component LOQ.

4.10 α-tocopherol

Vitamin E, or α-tocopherol, has these results after the analysis:

- Average Rt: 33.74 minutes.
- LOD $\leq$ 2.5 ppm.
- LOQ: 25 ppm.
- Average Response Factor: 1.7372.

Following concentrations of α-tocopherol were being analysed: 2.5 ppm, 5 ppm, 10 ppm, 25 ppm, 50 ppm, 100 ppm, 250 ppm, 500 ppm, 1000 ppm and 2500 ppm. Based on the chromatograms that GC-FID generated, the signals remained in symmetrical shape from 2.5 ppm until 100 ppm. From 250 ppm the peaks started to fronting.

A 10 points calibration curve with its equation and R^2 was constructed using given results.

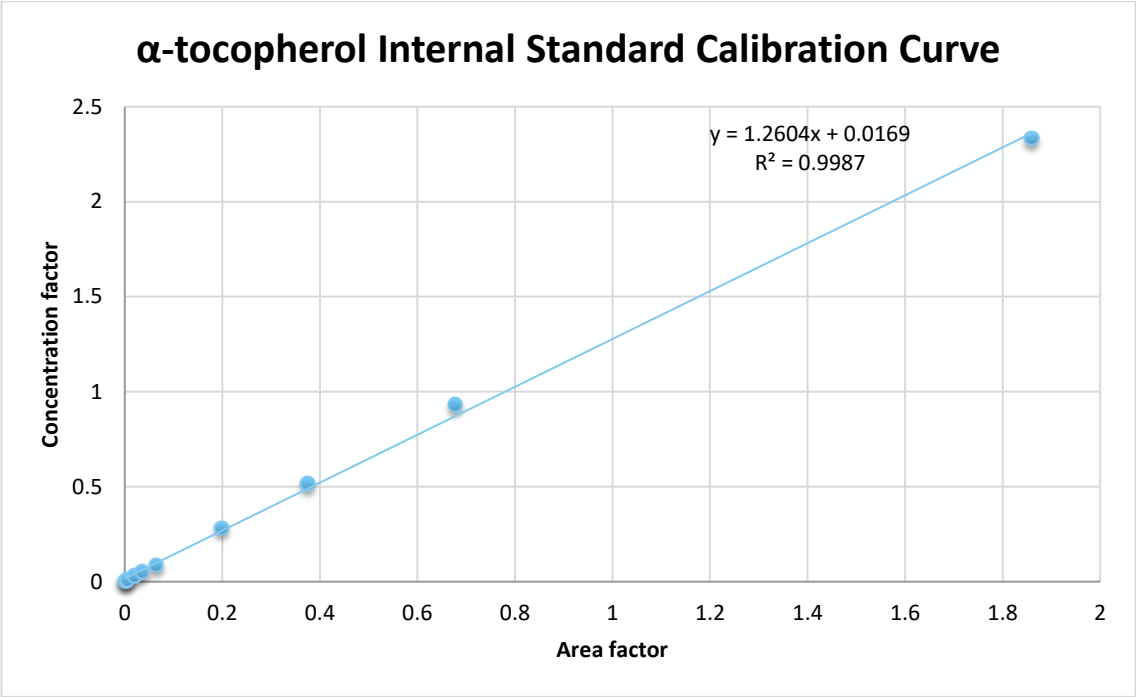

FIGURE 23. α-tocopherol Calibration Curve.

The table below reveal an overall peak area factor, theoretical and reality concentration factor plus their relative differences together with average Rt at each concentration.

TABLE 13. α-tocopherol overall results.

ppm	Corrected area factor	Reality concentration factor	Theoretical concentration factor (y)	Relative difference (%)	Average Rt (minutes)
2.5	0.0008	0.0027	0.0179	84.72	33.67
5	0.0036	0.0060	0.0214	71.98	33.66
10	0.0052	0.0105	0.0235	55.52	33.64
25	0.0200	0.0319	0.0421	24.27	33.64
50	0.0360	0.0539	0.0622	13.34	33.67
100	0.0652	0.0876	0.0990	11.60	33.69
250	0.1990	0.2821	0.2678	5.35	33.74
500	0.3745	0.5161	0.4889	5.56	33.79
1000	0.6776	0.9309	0.8710	6.88	33.86

2500	1.8600	2.3332	2.3612	1.19	33.98

TABLE 13 shows that average Rt increased from 33.64 minutes to 33.98 minutes along with concentration. At 25 ppm, the relative difference between theoretical concentration factor and the reality one is 24.27%, smaller than 30%, therefore 25 ppm is the component LOQ.

4.11 DL-α-palmitin

The results show that DL-α-palmitin has:

- Average Rt: 23.53.
- LOD: 25 ppm.
- LOQ: 50 ppm.
- Average Response Factor: 3.2189.

Following concentrations of DL-α-palmitin were being analysed: 2.5 ppm, 5 ppm, 10 ppm, 25 ppm, 50 ppm, 100 ppm, 250 ppm, 500 ppm, 1000 ppm and 2500 ppm. Based on the chromatograms that GC-FID generated, the peaks were un-detectable at the first three concentration. There were symmetrical shapes from 25 ppm to 250 ppm, the peaks started to show fronting at 500 ppm.

A 7 points calibration curve with its equation and R^2 was constructed using given results.

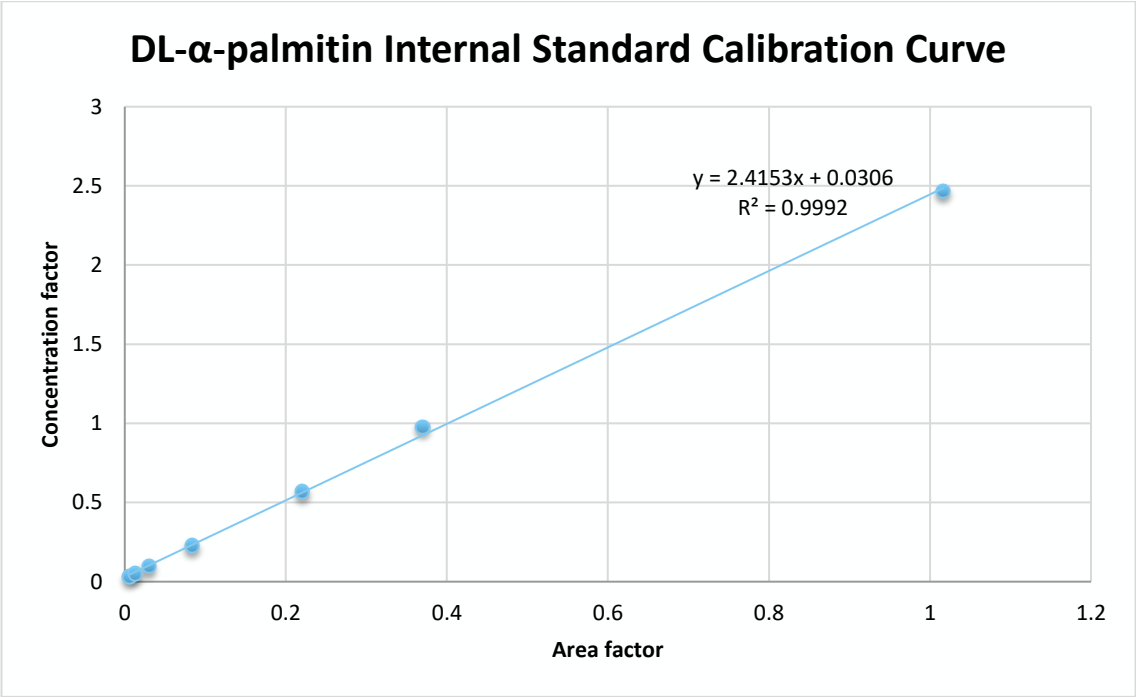

FIGURE 24. DL-α-palmitin Calibration Curve.

The table below reveal an overall peak area factor, theoretical and reality concentration factor plus their relative differences together with average Rt at each concentration.

TABLE 14. DL-α-palmitin overall results.

ppm	Corrected area factor	Reality concentration factor	Theoretical concentration factor (y)	Relative difference (%)	Average Rt (minutes)
25	0.0061	0.0311	0.0453	31.38	23.28
50	0.0130	0.0504	0.0621	18.92	23.30
100	0.0302	0.0964	0.1036	6.91	23.34
250	0.0839	0.2285	0.2333	2.07	23.43
500	0.2206	0.5682	0.5635	0.85	23.58
1000	0.3699	0.9762	0.9240	5.65	23.71
2500	1.0165	2.4667	2.4858	0.77	24.07

TABLE 14 shows that average Rt increased from 23.28 minutes to 24.07 minutesalong with concentration. At 50 ppm, the relative difference between

theoretical concentration factor and the reality one is 18.92%, smaller than 30%, therefore 50 ppm is the component LOQ.

4.12 TAGs mixture

Following concentrations of TAGs mixture were being analysed: 2.5 ppm, 5 ppm, 10 ppm, 25 ppm, 50 ppm, 100 ppm, 250 ppm, 500 ppm, 1000 ppm and 2500 ppm. There are 5 TAGs presented: tricaprylin, tricaprin, trilaurin, trimyristin and tripalmitin; each of which accounted for approximately 20% of the solution. Hence, each components were being analysed at 0.5 ppm, 1 ppm, 2 ppm, 5 ppm, 10 ppm, 20 ppm, 50 ppm, 100 pmm, 200 ppm and 500 ppm. The average theoretical RF of 5 TAGs is 1.90182.

4.12.1 Tricaprylin

Tricaprylin was the first detected TAG in the mixture. Its results are:

- Average Rt: 32.14 minutes.
- LOD $\leq$ 0.5 ppm.
- LOQ: 10 ppm.
- Average Response Factor: 1.5469.

Based on the chromatograms that GC-FID generated, there were symmetrical shapes from 0.5 ppm to 50 ppm, the peaks started to show fronting at 100 ppm.

A 10 points calibration curve with its equation and R^2 was constructed using given results.

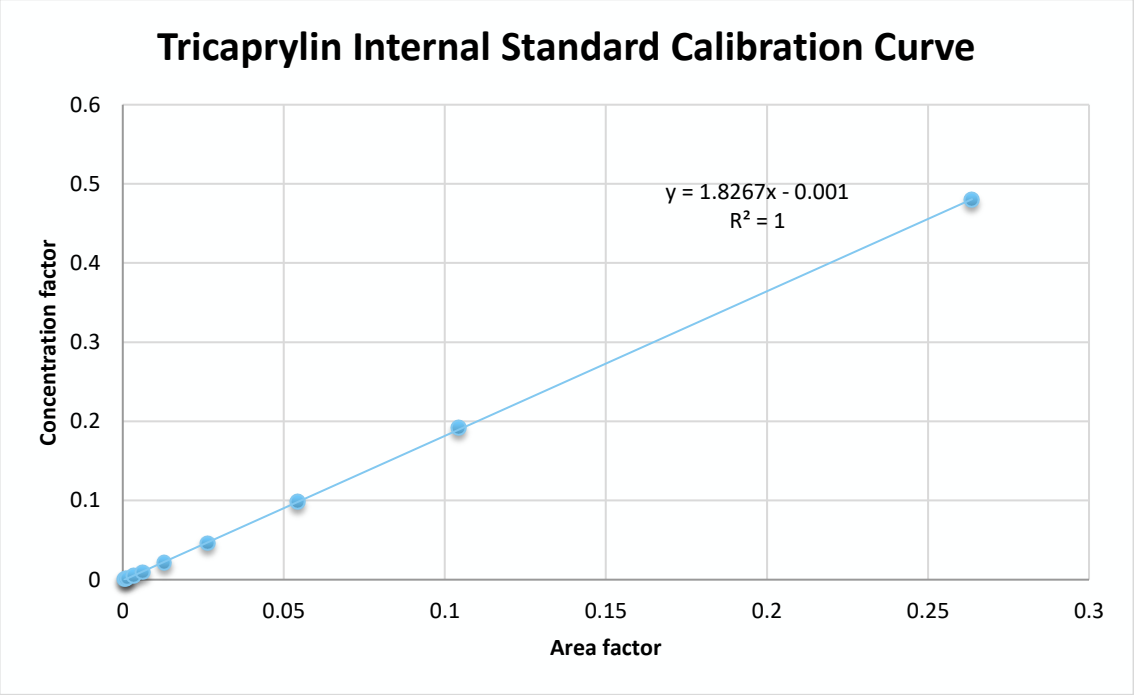

FIGURE 25. Tricaprylin Calibration Curve.

The table below reveal an overall peak area factor, theoretical and reality concentration factor plus their relative differences together with average Rt at each concentration.

TABLE 15. Tricaprylin overall results.

ppm	Corrected area factor	Reality concentration factor	Theoretical concentration factor (y)	Relative difference (%)	Average Rt (minutes)
0.5	0.0005	0.0005	0.0019	74.49	31.96
1	0.0009	0.0011	0.0027	58.06	31.96
2	0.0014	0.0019	0.0036	45.64	31.95
5	0.0034	0.0050	0.0072	30.42	31.94
10	0.0061	0.0094	0.0122	22.81	31.94
20	0.0129	0.0213	0.0245	12.96	31.95
50	0.0263	0.0461	0.0491	6.06	31.96
100	0.0543	0.0984	0.1002	1.80	31.99
200	0.1043	0.1919	0.1915	0.21	32.03

500	0.2637	0.4798	0.4827	0.58	33.71

TABLE 15 shows that average Rt increased from 31.94 minutes to 33.71 minutes along with concentration. At 10 ppm, the relative difference between theoretical concentration factor and the reality one is 22.81%, smaller than 30%, therefore 10 ppm is the component LOQ.

4.12.2 Tricaprin

The second peak in the chromatogram belongs to tricaprin. Its results are:

- Average Rt: 35.94 minutes.
- LOD ≤ 0.5 ppm.
- LOQ: 5 ppm.
- Average Response Factor: 1.4792.

Based on the chromatograms that GC-FID generated, there were symmetrical shapes from 0.5 ppm to 100 ppm, the peaks started to show fronting at 200 ppm.

A 10 points calibration curve with its equation and R^2 was constructed using given results.

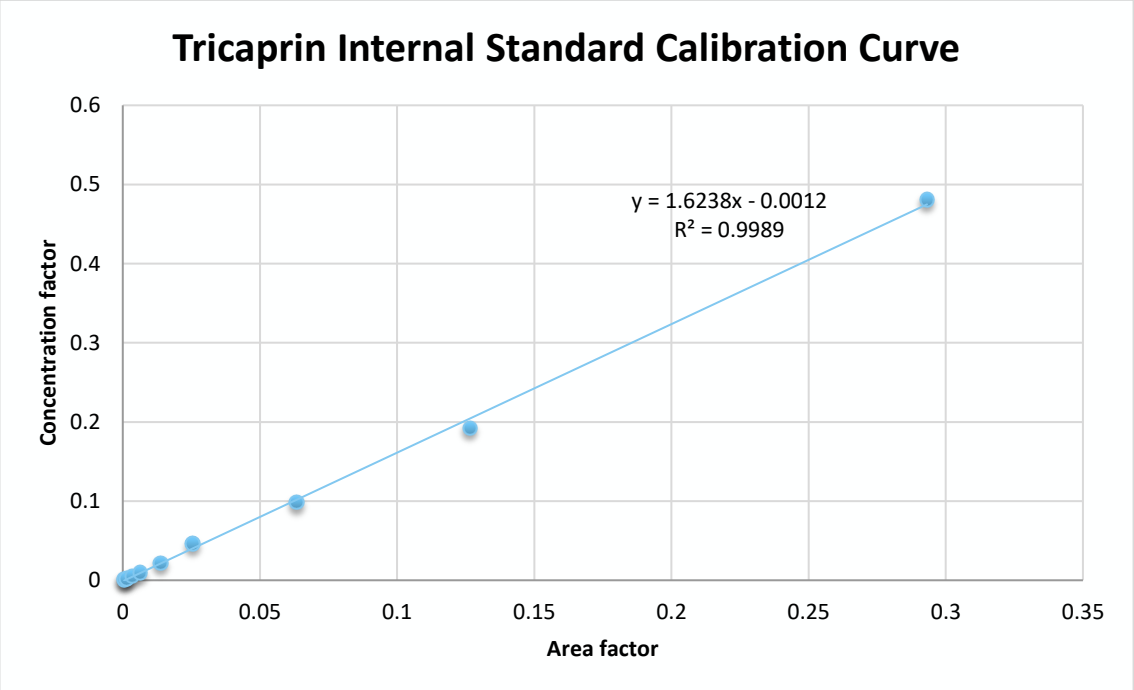

FIGURE 26. Tricaprin Calibration Curve.

The table below reveal an overall peak area factor, theoretical and reality concentration factor plus their relative differences together with average Rt at each concentration.

TABLE 16. Tricaprin overall results.

ppm	Corrected area factor	Reality concentration factor	Theoretical concentration factor (y)	Relative difference (%)	Average Rt (minutes)
0.5	0.0005	0.0005	0.0020	75.18	35.82
1	0.0006	0.0011	0.0022	49.09	35.81
2	0.0014	0.0019	0.0035	44.87	35.81
5	0.0034	0.0050	0.0067	25.56	35.81
10	0.0062	0.0094	0.0113	16.74	35.81
20	0.0138	0.0214	0.0237	9.73	35.81
50	0.0256	0.0462	0.0427	8.00	35.82
100	0.0633	0.0985	0.1040	5.31	35.83
200	0.1266	0.1921	0.2068	7.10	35.85
500	0.2932	0.4803	0.4772	0.64	37.08

TABLE 16 shows that average Rt increased from 35.81 minutes to 37. 08 minutes along with concentration. At 5 ppm, the relative difference between theoretical concentration factor and the reality one is 25.56%, smaller than 30%, therefore 5 ppm is the component LOQ.

4.12.3 Trilaurin

Trilaurin has the third peak in the chromatograms, the statistics of it are:

- Average Rt: 38.06 minutes.
- LOD ≤ 0.5 ppm.
- LOQ: 5 ppm.
- Average Response Factor: 1.5916.

Based on the chromatograms that GC-FID generated, there were symmetrical shapes from 0.5 ppm to 100 ppm, the peaks started to show fronting at 200 ppm.

A 10 points calibration curve with its equation and R^2 was constructed using given results.

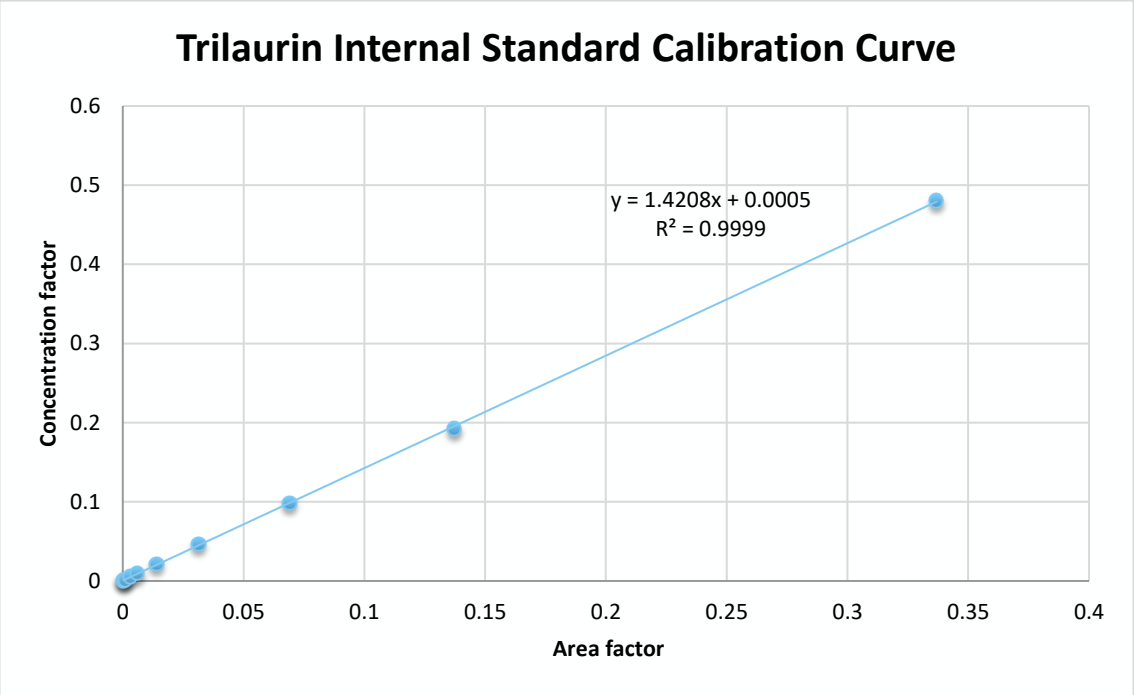

FIGURE 27. Trilaurin Calibration Curve.

The table below reveal an overall peak area factor, theoretical and reality concentration factor plus their relative differences together with average Rt at each concentration.

TABLE 17. Trilaurin overall results.

ppm	Corrected area factor	Reality concentration factor	Theoretical concentration factor (y)	Relative difference (%)	Average Rt (minutes)
0.5	0.0002	0.0005	0.0008	41.36	37.94
1	0.0005	0.0011	0.0013	12.60	37.94
2	0.0010	0.0019	0.0019	2.13	37.94
5	0.0030	0.0050	0.0048	3.20	37.93

10	0.0061	0.0094	0.0091	3.53	37.93
20	0.0140	0.0214	0.0204	4.82	37.93
50	0.0314	0.0462	0.0451	2.32	37.95
100	0.0690	0.0985	0.0985	0.03	37.96
200	0.1373	0.1921	0.1955	1.73	37.98
500	0.3369	0.4803	0.4791	0.25	39.14

TABLE 17 shows that average Rt increased from 37.93 minutes to 39.14 minutes along with concentration. At 1 ppm, the relative difference between theoretical concentration factor and the reality one is 12.60%, smaller than 30%, therefore 1 ppm is the component LOQ.

4.12.4 Trimyristin

The forth detected TAG was trimyristin. The results show that trimyristin has:

- Average Rt: 39.80 minutes.
- LOD: 2 ppm.
- LOQ: 5 ppm.
- Average Response Factor: 2.6596.

Based on the chromatograms that GC-FID generated, the peaks were undetectable at the first two concentration. There were symmetrical shapes from 2 ppm to 100 ppm, the peaks started to show fronting at 200 ppm.

An 8 points calibration curve with its equation and R^2 was constructed using given results.

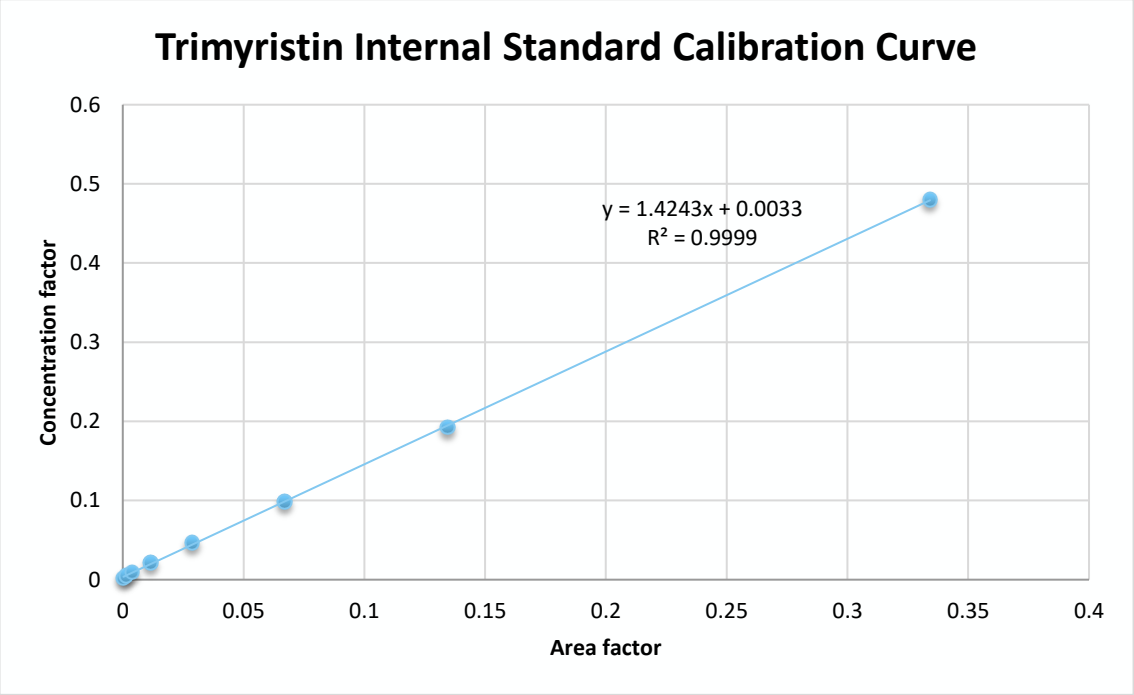

FIGURE 28. Trimyristin Calibration Curve.

The table below reveal an overall peak area factor, theoretical and reality concentration factor plus their relative differences together with average Rt at each concentration.

TABLE 18. Trimyristin overall results.

ppm	Corrected area factor	Reality concentration factor	Theoretical concentration factor (y)	Relative difference (%)	Average Rt (minutes)
2	0.0003	0.0019	0.0037	47.05	39.65
5	0.0014	0.0050	0.0054	7.04	39.64
10	0.0038	0.0094	0.0087	9.01	39.64
20	0.0116	0.0214	0.0198	8.12	39.64
50	0.0287	0.0462	0.0441	4.62	39.65
100	0.0670	0.0985	0.0987	0.23	39.67
200	0.1346	0.1921	0.1951	1.51	39.69
500	0.3342	0.4803	0.4793	0.21	40.85

TABLE 18 shows that average Rt increased from 39.64 minutes to 40.85 minutes along with concentration. At 5 ppm, the relative difference between theoretical concentration factor and the reality one is 7.04%, smaller than 30%, therefore 5 ppm is the component LOQ.

4.12.5 Tripalmitin

Tripalmitin was last detected in the mixture. According to the analysis, tripalmitin has:

- Average Rt: 41.33.
- LOD: 5 ppm.
- LOQ: 20 ppm.
- Average Response Factor: 3.1357.

Based on the chromatograms that GC-FID generated, the peaks were undetectable at the first three concentration. There were symmetrical shapes from 5 ppm to 200 ppm, the peaks started to show fronting at 500 ppm.

A 7 points calibration curve with its equation and R^2 was constructed using given results.

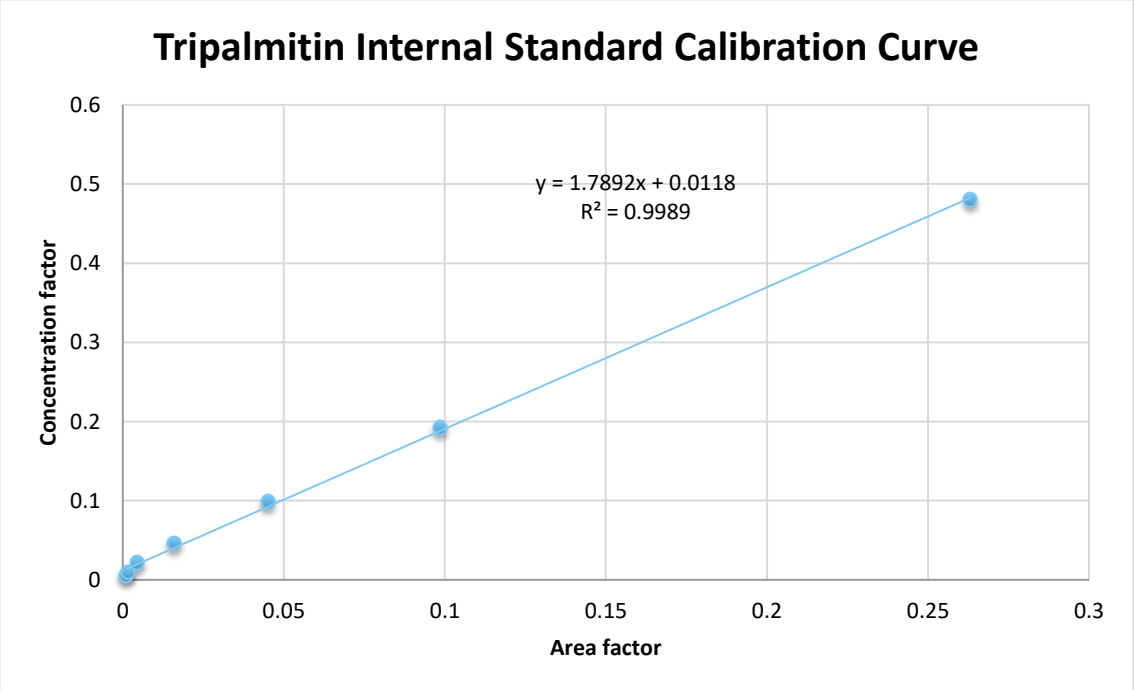

FIGURE 29. Tripalmitin Calibration Curve.

The table below reveal an overall peak area factor, theoretical and reality concentration factor plus their relative differences together with average Rt at each concentration.

TABLE 19. Tripalmitin overall results.

ppm	Corrected area factor	Reality concentration factor	Theoretical concentration factor (y)	Relative difference (%)	Average Rt (minutes)
5	0.0011	0.0050	0.0137	63.77	41.15
10	0.0017	0.0094	0.0148	36.16	41.15
20	0.0046	0.0213	0.0200	6.58	41.15
50	0.0159	0.0461	0.0403	14.37	41.16
100	0.0451	0.0984	0.0926	6.31	41.17
200	0.0986	0.1919	0.1882	1.97	41.19
500	0.2631	0.4798	0.4826	0.57	42.35

TABLE 19 shows that average Rt increased from 41.15 minutes to 42.35 minutes along with concentration. At 20 ppm, the relative difference between theoretical concentration factor and the reality one is 6.58%, smaller than 30%, therefore 20 ppm is the component LOQ.

5 DISCUSSION

The results have confirmed the sensitivity and efficiency of GC-FID in detecting oil components because it can identify such a wide range of analytes concentrations in an incredible accuracy. As the LOD and LOQ show, our method can reveal the methyl esters at around 0.5 ppm and other substances at around 2.5 ppm. The methyl esters also have the biggest quantification range, from around 2.5 ppm to over 1000 ppm. The only exception is methyl oleate with LOQ of 10 ppm. This might be the consequence of some GC failures. The fatty acids' quantification ranges are slightly smaller, begin from 10 ppm. The largest LOD is 25 ppm. This LOD belongs to α-tocopherol, which is a type of vitamin E; DL-α-palmitin, a monoacylglycerol; and tripalmitin, a TAG. The differences in LOD can be explained by the constituents polarity. Since the GC column polarity is low, it is more sensitive to small polarity substances like the methyl esters. Moreover, high volatility of methyl esters also help them acquire a wide detection range in GC-FID analysis (Cruz-Hernandez et al. 2016). Bigger RF value also indicate higher detection limit. Since RF is the correlation between concentration and area, the smaller the signal area (leads to larger LOD), the bigger RF get. Results of 5 TAGs proved this statement. The RF of tricaprylin, tricaprin, trilaurin, trimyristin, tripalmitin increase respectively, along with their LOD value. Beside that, Rt increses when concentration increases.

It is noticeable that from around 100 ppm to 250 ppm and over, the peaks of each component is starting to show fronting. This might be the result of overloading the column with sample. In case of the fatty acids, small concentration from 10 ppm and under generated tailing peaks. It can indicate bad chromatography due to sample insufficient. The chromatography of these peaks can be optimized by adjusting injection volume; however the quantitative statistics were still accurate so it is not necessary. Unfortunately, split peaks appeared in all methyl oleate analyses and stearic acid analyses from 10 ppm to 50 ppm. This peculiar shape was the effect of poor injection actions since the needle was blocked. This might also explain why methyl oleate results did not align with other esters data. After changing the needle of the injector, the chromatograms peaks were symmetrical again.

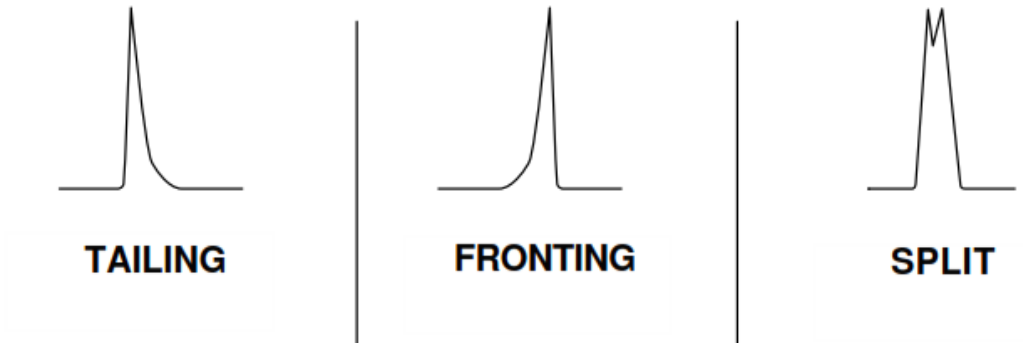

FIGURE 30. Irregular peak shapes (Instrumentation Forum)

The precision of final data also emphasizes the importance of IS. During the experiments, sometimes problems did occur: not enough sample injected or fluctuate flow rates (when there were problems with carrier flow, purge flow, split flow, make-up and detector gases, etc.), which led to abnormal data recorded. Such factors make it difficult to achieve the assumption required by external calibration-a method calls for identity in every single run. Internal calibration effectively eliminates these issues, by relying not on absolute values of detector response, but rather on response ratios between the peak area of analytes and peak area of IS. Because both substances receive the same treatment in the analysed sample, the ratio of their signal is not affected by any lack of reproducibility in the procedure. These proportions are extremely beneficial in building a reliable quantitative method. Inconsistent repeatability of injections were also the reason why the calculated average RF were slightly different from the slopes of calibration curves, which are the theoretical RF in an ideal analyzing model. The differences are also the results of many minor faults in dilution, computer, mobile and stationary phase of GC, etc. During the TAGs mixture analyse, there were column bleedings starting at around 39 minutes. This is the result of overheating the column, which leads to some material in the stationary phase coming out into the detector. Those bleedings caused difficulties in intergrating the peaks of trimyristin and tripalmitin, whose Rt are after 39 minutes. As a consequence, these components' reality RF were noticeably bigger than their theoretical RF.

Because of time restriction, the calibration could not be fully finished as planned. There are still some predominant components of oils such as longer-carbon-chain-TAGs, DAGs, MAGs, plant sterols and other types of tocopherols remain undone. If I was able to calibrate mixtures of several standards, it would be easier

to identify them separately in the chromatograms. Nevertheless, the final outcomes are valuable contributions to the progress of ExtReMo project.

6 CONCLUSION

Despite time limitation, I was successful in calibrating 16 oil constituents. The comprehensive results are displayed in TABLE 20 beneath. However, there are several other important components and stages more involved in order to complete a quantitative analysis of specialty oils using GC-FID.

TABLE 20. Analytical parameters of standards

	Calibration curve equation	R^2	Average RF	Average Rt (minutes)	LOD (ppm)	LOQ (ppm)
Methyl Palmitate	y = 1.2847x + 0.0003	0.9999	1.8380	15.03	0.5	2.5
Palmitic Acid	y = 1.7804x + 0.0067	0.9992	3.2849	15.42	2.5	10
Methyl Linoleate	y = 1.3159x - 0.0011	0.9999	1.1588	17.04	0.5	10
Methyl Oleate	y = 1.5074x - 0.0028	0.9994	1.1366	17.08	0.5	25
Methyl Stearate	y = 1.2622x + 0.0032	0.9983	1.2875	17.52	0.25	10
Linoleic Acid	y = 2.7649x + 0.0117	0.9975	5.2979	17.62	2.5	10
Oleic Acid	y = 1.4478x + 0.0068	0.9995	3.5855	17.70	2.5	10
Stearic Acid	y = 1.5235x + 0.0155	0.9986	4.1173	18.08	5	25
DL-α-palmitin	y = 2.4153x + 0.0306	0.9992	3.2189	23.53	25	50
Squalene	y = 1.1646x + 0.01	0.9965	1.1439	30.30	2.5	50
Tricaprylin	y = 1.8267x + 0.001	1	1.5469	32.14	0.5	10
α-tocopherol	y = 1.2604x + 0.0169	0.9987	1.7372	33.74	2.5	25

Tricaprin	y = 1.6238x + 0.0012	0.9989	1.4792	35.94	0.5	5
Trilaurin	y = 1.4208x + 0.0005	0.9999	1.5916	38.06	0.5	1
Trimyristin	y = 1.4243x + 0.0033	0.9999	2.6596	39.80	2	5
Tripalmitin	y = 1.7892x + 0.0118	0.9989	3.1357	41.33	5	20

REFERENCES

Anderson, S. 2004. Soxtec: Its Principles and Applications. Oil Extraction and Analysis: Critical Issues and Comparative Studies. Luthria, D.L. (Ed). Routledge, New York, 23.

Augustsson, K. 2003. A prospective study of intake of fish and marine fatty acids and prostate cancer. Cancer Epidemiology, Biomarkers & Prevention 12 (1), 64–67.

Awad, A.B. & Fink, C.S. 2000. Phytosterols as anticancer dietary components: evidence and mechanism of action. J. Nutr. 130, 2127– 2130.

Bamgboye, A. & Adejumo, A. 2007. Development of a sunflower oil expeller. Agricultural Engineering International: the CIGR E-journal. Manuscript EE 06 015, vol IX.

Bhupathiraju, S.N. & Tucker, K.L. 2011. Coronary heart disease prevention: nutrients, foods, and dietary patterns. Clin. Chim. Acta 412, 1493– 1514.

Bruckert, E. & Rosenbaum, D. 2011. Lowering LDL-cholesterol through diet: potential role in the statin era. Curr. Opin. Lipidol. 22, 43– 48.

Bucher, H. C., Hengstler, P., Schindler, C. & Meier, G. 2002. n−3 polyunsaturated fatty acids in coronary heart disease: a meta–analysis of randomized controlled trials. Am J Med 112 (4), 298–304.

Burlingame, A.L., Boyd, R.K. & Gaskell, S.J.1998. Mass Spectrometry. Anal. Chem. 70, 647R.

Burr M. L., Sweetham P. M., Fehily A. M. 1994. Diet and reinfarction. European Heart Journal 15 (8), 1152–1153.

Calder, P.C. 2006. n−3 polyunsaturated fatty acids, inflammation, and inflammatory diseases. American Journal of Clinical Nutrition 83 (6), 1505–1519.

Caygill, C. P., Hill M. J. 1995. Fish, n−3 fatty acids and human colorectal and breast cancer mortality. Eur J Cancer Prev 4 (4), 329–332.

Choe, E. & Min, D.B., 2006. Mechanisms and factors for edible oil oxidation. Compr. Rev. Food Sci. Food Saf. 5, 169– 186.

Corma, A., Hamid, S.B.A., Iborra, S. & Velty, A. 2005. Lewis and Bronsted basic active siteson solid catalysts and their role in the synthesis of monoglycerides. J Catal 234: 340-347.

Cruz-Hernandez, C., Destaillats. F. 2016. Gas Chromatography of Fatty Acid Methyl Esters: Derivatization. Encyclopedia of Lipidomics. Springer.

Deckere, E.A. 1999. Possible beneficial effect of fish and fish n−3 polyunsaturated fatty acids in breast and colorectal cancer. Eur J Cancer Prev 8 (3), 213–221.

Dennis, K.J. & Shibamoto, T. 1989. Production of malonaldehyde from squalene, a major skin surface lipid during UV-irradiation. Photochem. Photobiol. 49, 711–716.

Dudley, K.H., Pippenger, C.E., Panry, J.K. & Kutt, H. 1978. Antiepileptic Drugs: Quantitative analysis and interpretation. Raven Press. New York.

Dunford, N., 2016. Oil and Oilseed Processing II. Robert M. Kerr Food & Agricultural Products Center, FAPC-159.

Eder, K. 1995. Gas chromatographic analysis of fatty acid methyl esters. Journal of Chromatography B 671, 113–131.

Engin, K.N., Engin, G., Kucuksahin, H., Oncu, M., Guvener, B. 2007. Clinical evaluation of the neuroprotective effect of alpha-tocopherol against glaucomatous damage. Eur. J. Ophthalmol. 17, 528– 533.

Eskin, N.A.M. 2008. Borage and evening primrose oil. European Journal of Lipid Science adnd Technololgy. 110, 651– 654.

European Medicines Agency. 2011. Guideline on bioanalytical method validation, 9-10.

Ferchau, E. 2000. Equipment of Decentralized Cold Pressing of Oil Seeds, Webpage of Folkecenter For Renewable Energy, www.folkecenter.dk, 19.

Fernholz, E. 1938. On the constitution of α -tocopherol. J. Am. Chem. Soc. 60, 700– 705.

Flickinger, B.D. & Matsuo, N. 2003. Nutritional characteristics of DAG oil". Lipids. 38 (2), 129–132.

Frank, J. 2004. Dietary phenolic compounds and vitamin E bioavailability. Model studies in rats and humans. Ph.D. thesis, Swedish University of Agricultural Sciences.

Frankel, E.N., Satué-Gracia, T., Meyer, A.S. & German, J.B. 2002. Oxidative stability of fish and algae oils containing long-chain polyunsaturated fatty acids in bulk and in oil-in-water emulsions. J. Agric. Food Chem. 50, 2094– 2099.

Gaonkar, R., Yallappa, S., Dhananjaya, B.L & Hegde, G. 2016. Development and validation of reverse phase high performance liquid chromatography for citral analysis from essential oils. Journal of Chromatography B, vol. 1036-1037, 50–56.

Ghanbari, R., Anwar, F., Alkharfy, K.M., Gilani, A.-H., Saari, N. 2012. Valuable nutrients and functional bioactives in different parts of olive (Olea europaea L.)—a review. Int. J. Mol. Sci. 13, 3291– 3340.

Grimes, D.S. Hindle, E. & Dyer, T. 1996. Sunlight, cholesterol and coronary heart disease. Q. J. Med. 89, 579– 590.

Hammond, E.W. 2003. Encyclopedia of Food Sciences and Nutrition, 2nd ed. VEGETABLE OIL- Types and properties. Academic Press, 5899.

Harris, D. C. 2007. Quantitative Chemical Analysis, 7th ed. W. H. Freeman and Company. New York, 109.

Harvey, D. 2016. Modern Analytical Chemistry. 3rd ed. McGraw-Hill Companies, 54.

Hensley, K., Benaksas, E.J., Bolli, R., Comp, P., Grammas, P., Hamdheydari, L., Mou, S., Pye, Q.N., Stoddard, M.F., Wallis, G., Williamson, K.S., West, M., Wechter, W.J., Floyd, R.A. 2004. New perspectives on vitamin E: γ -tocopherol and carboxyethylhydroxychroman metabolites in biology and medicine. Free Radic. Biol. Med. 36, 1– 15.

Hibbeln, J.R. 2006. Healthy intakes of n−3 and n−6 fatty acids: estimations considering worldwide diversity. American Journal of Clinical Nutrition 83 (6), 1483–1493.

https://www.ck12.org/c/chemistry/triglycerides/lesson/Triglycerides-CHEM/, Read:08/05/2020.

Huber, L. 2007. Validation and Qualification in Analytical Laboratories (2), 144–211.

Illum, R. F., Mussolino, M. E., Madans, J. H. 1996. The relationship between fish consumption and stroke incidence: The NHANES I Epidemiologic Follow–up Study (National Health and Nutrition Examination Survey. Arch Intern Med 156 (5), 537–542.

Instrumentation Forum. 2019. Gas Chromatograph (GC) Tuning. https://instrumentationforum.com/t/gas-chromatograph-gc-tuning/9000/2. Read: 12/05/2020.

Iso, H., Rexrode, K. M., Stampfer, M. J., Manson, J. E., Colditz, G. A., Speizer, F. E., Hennekens, C. H. & Willett, W. C. 2001. Intake of fish and omega–3 fatty acids and risk of stroke in women. JAMA 285 (3), 304–312.

IUPAC. 1987. Standard methods for analysis of oils, fats and derivatives. Blackwell Scientific Publications, 7th ed. IUPAC method 2.301. Report of IUPAC Working Group WG 2/87.

Jones, P.J.H. & AbuMweis, S.S. 2009. Phytosterols as functional food ingredients: linkages to cardiovascular disease and cancer. Curr. Opin. Clin. Nutr. Metab. Care 12, 147– 151.

Jung, M.Y.& Min, D. 2005. Novel hydrogenation for low trans fatty acids in vegetable oils. Healthful Lipids. AOCS Press. Champaign IL, 65-77.

Kamal-Eldin, A. & Hernandez, E.M. 2013. Processing and Nutrition of Fats and Oils. IFT Press. WILEY Blackwell. Texas, 53, 226.

Kenar, J.A. & Moser, B.R. & List, G.R. 2017. Naturally Occuring Fatty Acids: Source, Chemistry, and Uses. FATTY ACIDS: Chemistry, Synthesis, and Applications, Ahmad, M.U. (ed). AOCS Press. Elsevier Inc. United Kingdom, 39-43.

Kornsteiner, M., Wagner, K.-H. & Elmadfa, I., 2006. Tocopherols and total phenolics in 10 different nut types. Food Chem. 98, 381– 387.

Kritchevsky, D., Chen, S.C. 2005. Phytosterols— health benefits and potential concerns: a review. Nutr. Res. 25, 413– 428.

Lands W. E. M. 2005. Dietary fat and health: the evidence and the politics of prevention: careful use of dietary fats can improve life and prevent disease. Annals of the New York Academy of Sciences 1055, 179–192.

Lu, T., Harper, A.F., Zhao, J. & Dalloul, R.A., (2014) Effects of a dietary antioxidant blend and vitamin E on growth performance, oxidative status, and meat quality in broiler chickens fed a diet high in oxidants. Poult. Sci. 93, 1– 9.

Maguire, L.S., O'Sullivan, S.M., Galvin, K., O'Connor, T.P., O'Brien, N.M., 2004. Fatty acid profile, tocopherol, squalene and phytosterol content of walnuts, almonds, peanuts, hazelnuts and the macadamia nut. Int. J. Food Sci. Nutr. 55, 171– 178.

Mandal, S.C, Mandal, V. & Das, A.K. 2015. Essentials in Botanical Extraction, Academic Press, 83-88.

Maranz, S. & Wiesman, Z. 2004. Influence of climate on the tocopherol content of shea butter. J. Agric. Food Chem. 52, 2934– 2937.

Mariana, I., Nicoleta, U., Sorin-Ştefan, B., Gheorghe,V. & Mirela, D. 2013. Actual methods for obtaining vegetable oil from oilseeds, University of Bucharest, Department of Biotechnical Systems, 3.

Mir, F., Rather, M.A., Dar, B.A. 2012. Comparative GC-FID and GC-MS analysis of the chemical profile of the leaf, stem and root essential oils of Artemisia dracunculus L. growing in Kashmir (India). Journal of Pharmaceutical Research, vol. 5, no. 3, 1353–1356.

Morris, M.C., Evans, D.A., Tangney, C.C., Bienias, J.L., Wilson, R.S., Aggarwal, N.T., Scherr, P.A. 2005. Relation of the tocopherol forms to incident Alzheimer disease and to cognitive change. Am. J. Clin. Nutr. 81, 508– 514.

Muti, P., Awad, A.B., Schünemann, H., Fink, C.S., Hovey, K., Freudenheim, J.L., Wu, Y.-W.B., Bellati, C., Pala, V., Berrino, F. 2003. A plant food– based diet modifies the serum β -sitosterol concentration in hyperandrogenic postmenopausal women. J. Nutr. 133, 4252– 4255.

Nelson, D. L.& Cox, M. M. 2000. Lehninger Principles of Biochemistry. 3rd ed. New York: Worth Publishing.

O'Brien, R. 1998. Fats and Oils. Formulating and Processing Applications.Technomic Publishing.

Owen, R.W., Giacosa, A., Hull, W.E., Haubner, R., Würtele, G., Spiegelhalder, B., Bartsch, H. 2000. Olive-oil consumption and health: the possible role of antioxidants. Lancet Oncol. 1, 107– 112.

Papazova, D. & Pavlova, A. 1999. Development of a Simple Gas Chromatographic Method for Differentiation of Spilled Oils. Journal of Chromatographic Science, 37, 1-4.

Pappas, A. 2009. Epidermal surface lipids. Dermato-endocrinology. **1** (2), 72–76.

Pavia, L., Gary M. L., George S. K. & Randall G. E. 2006. Introduction to Organic Laboratory Techniques (4th Ed.). Thomson Brooks/Cole, 797–817.

Phleger, C.F. 1998. Buoyancy in marine fishes: direct and indirect role of lipids. Am. Zool. 38, 321– 330.

Pollack, A. 2009. Benefit and doubt in vaccine additive. New York Times, September 22.

Pollak, O.J. 1953. Successful prevention of experimental hypercholesteremia and cholesterol atherosclerosis in the rabbit. Circulation 7, 696– 701.

Quirós, R.B., Sanches–Silva, A, López– Hernández, J. 2004. Comparison between high–performance liquid chromatography and gas chromatography methods for fatty acid identification and quantification in potato crisps. Journal of Chromatography 1032 (1–2), 7–15.

Reddy, L.H., Couvreur, P. 2009. Squalene: a natural triterpene for use in disease management and therapy. Adv. Drug Deliv. Rev. 61, 1412– 1426.

Reina, R.J., White, K.D. & Firestone, D. 1999. Sterol and triterpene diol contents of vegetable oils by high-resolution capillary gas chromatography. J. AOAC Int. 82, 929– 935.

RESTEK. 2002. Operating Hints for Using Split/Splitless Injectors. Technical guide, United States, 22.

RESTEK. 2013. Guide to GC Column Selection and Optimizing Separations, United States, 6-9.

Richard, B. 2008. Bioethanol and bidiesel overview. WREC. Bangkok. Thailand.

Richfield, J. 2014. Monoacylglycerol -1 molecular structure, Wikimedia Commons, https://commons.wikimedia.org/wiki/File:Monoacylglycerol_-1_molecular_structure.jpg. Read: 10/05/2020.

Ripoll, G., Joy, M. & Muñoz, F., 2011. Use of dietary vitamin E and selenium (Se) to increase the shelf life of modified atmosphere packaged light lamb meat. Meat Sci. 87, 88– 93.

Rome, K. & McIntyre, A. 2012. Intelligent use of Relative Response Factors in Gas Chromatography-Flame Ionisation Detection. Chromatography Today, 52.

Ryan, E., Galvin, K., O'Connor, T.P., Maguire, A.R., O'Brien, N.M. 2006. Fatty acid profile, tocopherol, squalene and phytosterol content of brazil, pecan, pine, pistachio and cashew nuts. Int. J. Food Sci. Nutr. 57, 219– 228.

Saig, A. 2014. What Is the Difference Between Saturated and Unsaturated Fat, and What Are Trans Fats?. Davidson Institute of Science Education. https://davidson.weizmann.ac.il/en/online/askexpert/chemistry/what-difference-between-saturated-and-unsaturated-fat-and-what-are-trans-fats-eyal. Read:08/05/2020.

Sari, P. 2006. Preliminary design and construction of a prototype canola seed oil extraction machine. Ph.D. Thesis, Middle East Technical University, Ankara, Turkey.

Shantha N. C., Guillermo E. N. 1992. Gas chromatography of fatty acids. Journal of Chromatography A 624, 37–51.

Sheng, J. 2013. Triglycerides,

Signal Group. Flame Ionisation Detector. www.signal-group.com. Read: 07/05/2020

Siró, I., Kápolna, E., Kápolna, B., Lugasi, A. 2008. Functional food. Product development, marketing and consumer acceptance— a review. Appetite 51, 456–467.

Smith, R.V. & Stewart, J.T. 1981. Textbook of Biopharmaceutic Analysis, a Description of Methods for the Determination of Drugs. Biological Fluids; Treatment of Chromatographic Data. Lea & Febiger (Eds). Philadelphia.

Sonntag, Norman O.V. 1982. Glycerolysis of fats and methyl esters — Status, review and critique. Journal of the American Oil Chemists' Society. 59 (10), 795A–802A.

Soult, A., 2019. Lipids and Triglycerides. Chemistry LibreTexts, Read: 10/05/2020, https://chem.libretexts.org.

Speek, A.J., Schrijver, J., Schreurs, W.H.P. 1985. Vitamin E composition of some seed oils as determined by high - performance liquid chromatography with fluorometric detection. J. Food Sci. 50, 121– 124.

Stauffer, E., Dolan, J. A. & Newman, R. 2008. Fire Debris Analysis. Academic Press, 235

Su, K.P., Huang S.Y., Chiub C.C. & Shenc W.W. 2003. Omega–3 fatty acids in major depressive disorder: A preliminary double– blind, placebo–controlled trial. Eur Neuropsychopharmacol 13 (4), 267– 271.

Sugano, M., Tsuji, E. 1997. Rice bran oil and cholesterol metabolism. J. Nutr. 127, 521S– 524S.

Talbot, G. (Ed.). 2015. Specialty oils and fats in food and nutrition : Properties, processing and applications. Woodhead Publising. United Kingdom, 326, 331, 335.

Taylor, H.R., Tikellis, G., Robman, L.D., McCarty, C.A. & McNeil, J.J. 2002. Vitamin E supplementation and macular degeneration: randomised controlled trial. Br. Med. J. 325, 11– 16.

Thomas, A. 2002. Fats and Fatty Oils. Ullmann's Encyclopedia of Industrial Chemistry. Weinheim.

Traber, M.G. & Atkinson, J. 2007. Vitamin E, antioxidant and nothing more. Free Rad. Biol. Med. 43, 4– 15.

Wolosik, K., Knas, M., Zalewska, A., Niczyporuk, M.& Przystupa A.W. 2013. The importance and perspective of plant-based squalene in cosmetology. J Cosmet Sci. 2013 Jan-Feb;64(1), 59-66.

Woyengo, T.A., Ramprasath, V.R. & Jones, P.J.H. 2009. Anticancer effects of phytosterols. Eur. J. Clin. Nutr. 63, 813– 820.

Yang, X. & Boyle, R.A. 2016. Sensory Evaluation of Oils/Fats and Oil/Fat–Based Foods. Oxidative Stability and Shelf Life of Foods Containing Oils and Fats. Hu & Jacobsen (Eds). AOCS Press.

Zheng, Y., Chen, X. & Shen, Y. 2008. Commodity chemicals derived from glycerol, an important biorefinery feedstock. Chem Rev 108, 5253-5277.

APPENDICES

Appendix 1. Squalene chromatograms signals

ppm	1st injection		2nd injection		3rd injection		Concentration	
	Area IS	Area Std	Area IS	Area Std	Area IS	Area Std	IS in vial (g)	Std in vial (g)
2.5	1315.181	2.325	1271.055	2.161	1259.872	2.22	0.00102222	4.71237E-07
5	1258.809	4.872	1205.368	4.822	1161.393	4.684	0.00094669	1.31172E-06
10	1145.113	8.504	1146.077	8.596	1156.168	8.792	0.00117038	2.51051E-06
25	1047.255	22.841	1029.003	23.24	1024.812	22.731	0.00132469	5.22834E-06
50	1051.998	43.372	1081.835	43.94	1075.733	43.398	0.00116899	1.03813E-05
100	403.606	29.551	1060.208	87.771	1047.027	85.684	0.00125518	2.49795E-05
250	71.096	5.872	1122.976	194.72	1107.778	192.424	0.00116845	5.44334E-05
500	582.954	201.227	939.983	372.335	475.209	156.843	0.00123186	0.000103221
1000	19.825	11.737	96.308	32.056	920.413	650.898	0.00120507	0.000262626
2500	113.65	68.735	1012.233	1829.464	1138.827	2151.493	0.00124672	0.000498993

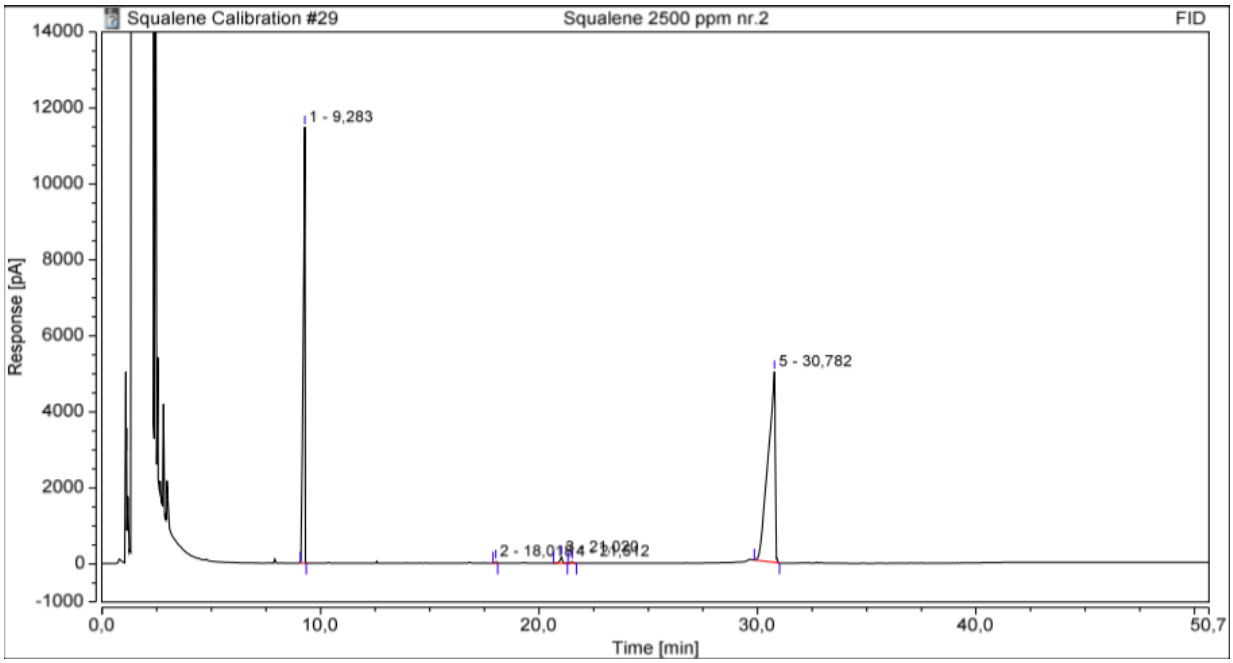

Squalene 2500 ppm chromatogram.

Appendix 2. Methyl Palmitate chromatograms signals

ppm	1st injection		2nd injection		3rd injection		Concentration	
	Area IS	Area Std	Area IS	Area Std	Area IS	Area Std	IS in vial (g)	Std in vial (g)
0.5	943.401	0.468	936.895	0.465	929.722	0.467	0.00102222	4.71237E-07
1	860.732	1.155	879.465	1.124	943.483	1.234	0.00094669	1.31172E-06
2.5	1132.551	1.974	1149.271	2.012	1186.628	2.025	0.00117038	2.51051E-06
5	1299.694	5.22	1184.804	4.811	1332.019	5.458	0.00132469	5.22834E-06
10	1103.631	8.026	1103.955	7.859	1120.934	8.054	0.00116899	1.03813E-05
25	1140.58	19.048	1249.03	21.19	1264.832	20.82	0.00125518	2.49795E-05
50	1224.296	44.323	1150.698	41.538	1182.294	42.082	0.00116845	5.44334E-05
100	1160.989	76.659	1203.905	81.443	1262.498	84.611	0.00123186	0.000103221
250	1185.359	196.71	1200.307	201.534	1199.448	194.482	0.00120507	0.000262626
500	333.352	98.015	1274.718	398.759	1273.551	401.048	0.00124672	0.000498993
1000	982.213	878.887	1129.571	1007.05	1066.034	961.901	0.00105174	0.001208631

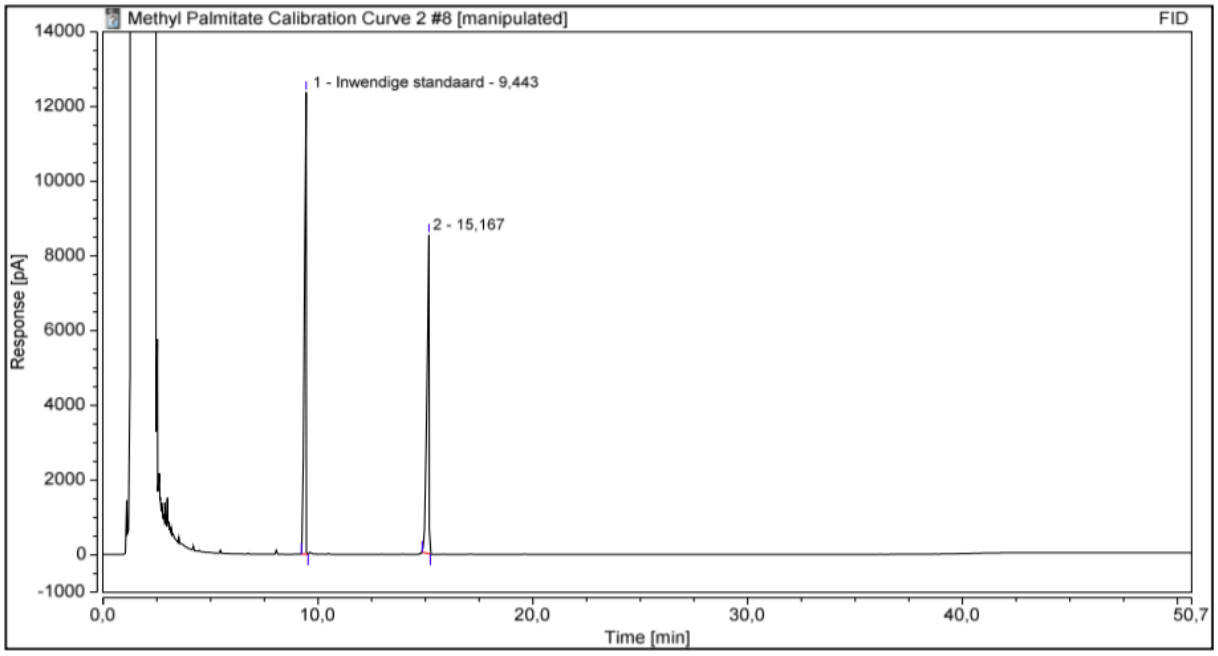

Methyl palmitate 1000 ppm chromatogram.

Appendix 3. Methyl Linoleate chromatograms signals

ppm	1st injection		2nd injection		3rd injection		Concentration	
	Area IS	Area Std	Area IS	Area Std	Area IS	Area Std	IS in vial (g)	Std in vial (g)
0.5	1076.065	0.576	1119.463	0.606	1181.621	0.63	0.00104305	5.08941E-07
1	1015.649	1.098	1032.109	1.056	992.94	1.094	0.00104277	1.02935E-06
2.5	1129.848	2.426	1094.022	2.282	1121.588	2.362	0.00105149	2.5695E-06
5	1175.918	5.3	1178.158	5.334	1152.567	5.224	0.00113239	5.14923E-06
10	966.5	10.008	998.378	10.417	958.384	9.908	0.00096552	1.15894E-05
25	1075.335	21.454	1169.754	23.299	1146.505	23.061	0.00110316	2.54013E-05
50	1054.502	42.806	1090.363	44.419	1036.134	42.127	0.00102108	5.06574E-05
100	1280.681	80.604	1277.355	78.466	1326.173	81.856	0.00127839	9.92761E-05
250	1077.452	190.362	1180.202	207.188	1103.066	186.537	0.00108213	0.000251403
500	1014.598	404.289	1039.267	407.026	1041.1	396.77	0.00099009	0.000510931
1000	1168.68	837.388	1291.151	897.999	499.795	342.262	0.00119881	0.001098004

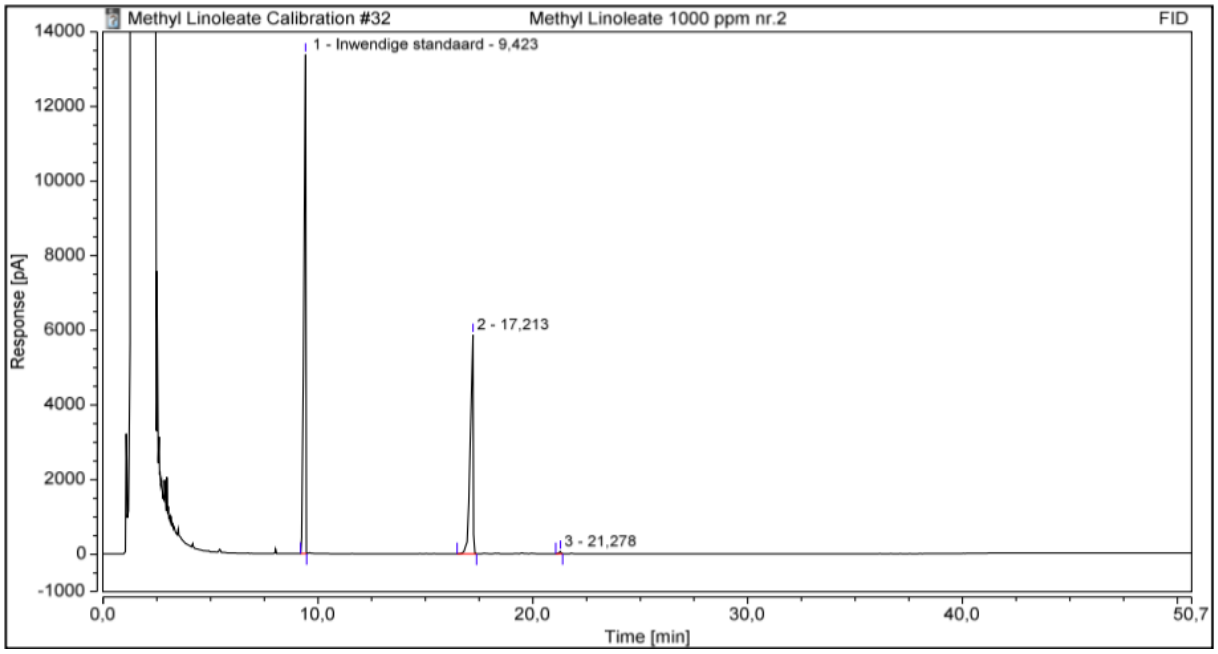

Methyl linoleate 1000 ppm chromatogram.

Appendix 4. Methyl Oleate chromatograms signals

ppm	1st injection		2nd injection		3rd injection		Concentration	
	Area IS	Area Std	Area IS	Area Std	Area IS	Area Std	IS in vial (g)	Std in vial (g)
0.25	99.145	0	916.288	0.537	940.128	0.566	0.00095408	2.43683E-07
0.5	953.537	0.713	1066.535	0.77	1013.368	0.71	0.00102152	4.96552E-07
1	1122.692	1.382	1013.029	1.394	996.944	1.324	0.00094681	9.98623E-07
2.5	1034.767	2.706	1005.141	2.704	960.986	2.582	0.00097705	2.58598E-06
5	1044.645	5.588	991.849	5.26	961.238	5.066	0.00090981	5.18795E-06
10	1092.332	10.393	1046.856	9.732	1000.514	9.364	0.00092718	1.03902E-05
25	1017.704	22.896	998.707	22.501	976.542	21.728	0.00092723	2.59332E-05
50	1033.36	41.244	979.468	40.089	1013.033	41.907	0.00091379	4.82897E-05
100	1095.398	84.782	1102.73	86.514	1048.863	81.215	0.00094702	9.83793E-05
250	421.275	65.144	420.355	65.454	267.002	39.814	0.0010267	0.000253562
500	978.093	335.313	1024.108	352.055	1017.69	346.48	0.00097641	0.000490235
1000	327.583	216.336	979.919	695.134	976.264	687.678	0.00094923	0.000989375

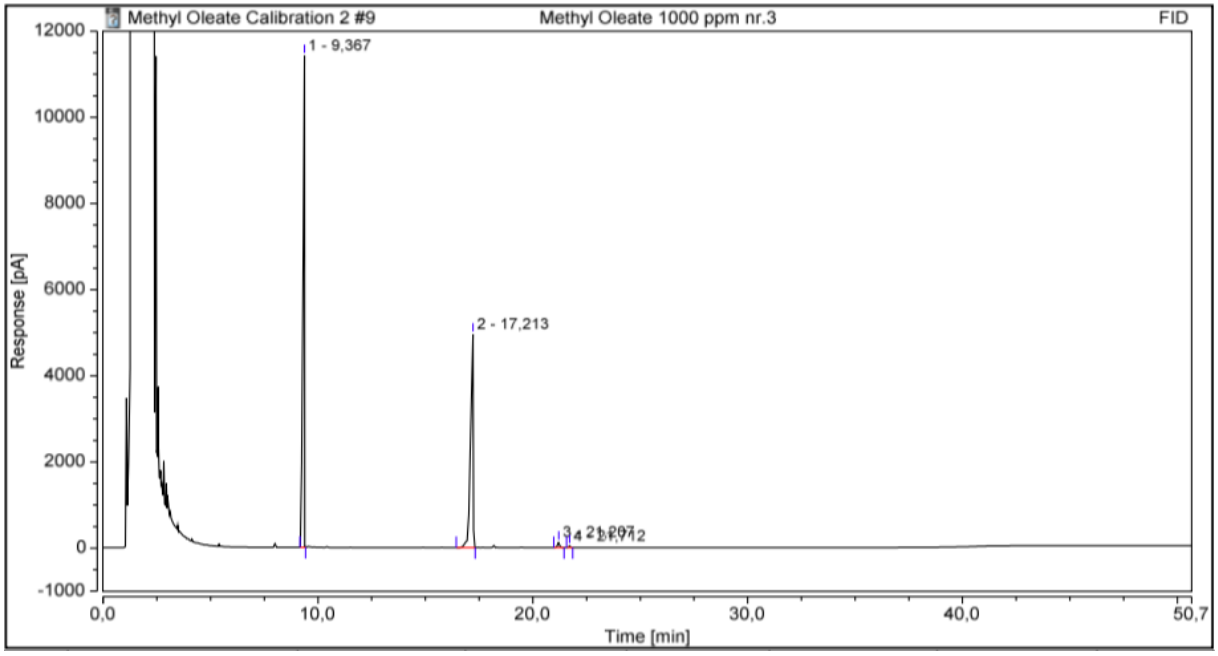

Methyl oleate 1000 ppm chromatogram.

Appendix 5. Methyl Stearate chromatograms signals

ppm	1st injection		2nd injection		3rd injection		Concentration	
	Area IS	Area Std	Area IS	Area Std	Area IS	Area Std	IS in vial (g)	Std in vial (g)
0.25	262.03	0.631	805.765	0.235	962.186	0.219	0.00094925	2.84736E-07
0.5	82.247	0.405	1004.304	0.381	1035.005	0.393	0.0009817	5.31702E-07
1	439.788	0.33	1132.407	0.808	1141.384	0.834	0.00110038	1.08028E-06
2.5	1126.817	2.076	1158.028	2.009	1139.699	2.042	0.00112819	2.53912E-06
5	1120.907	4.155	1145.445	4.224	1147.003	4.176	0.00108745	5.0255E-06
10	195.317	1.146	1121.974	8.515	1119.825	8.404	0.00103645	9.88944E-06
25	1110.877	23.105	1103.468	23.1	1087.66	22.098	0.00100945	2.54053E-05
50	1138.329	42.56	1139.831	43.168	1098.508	40.79	0.00103555	4.92731E-05
100	1131.944	84.577	1137.808	86.761	1107.886	82.351	0.00103995	9.98955E-05
250	1186.898	213.783	1149.318	203.08	1115.797	196.821	0.00111318	0.000269578
500	790.66	286.718	1114.5	395.937	1129.753	404.691	0.00101902	0.000495778
1000	1069.549	809.18	1054.447	770.066	1170.562	887.184	0.00106175	0.000987528

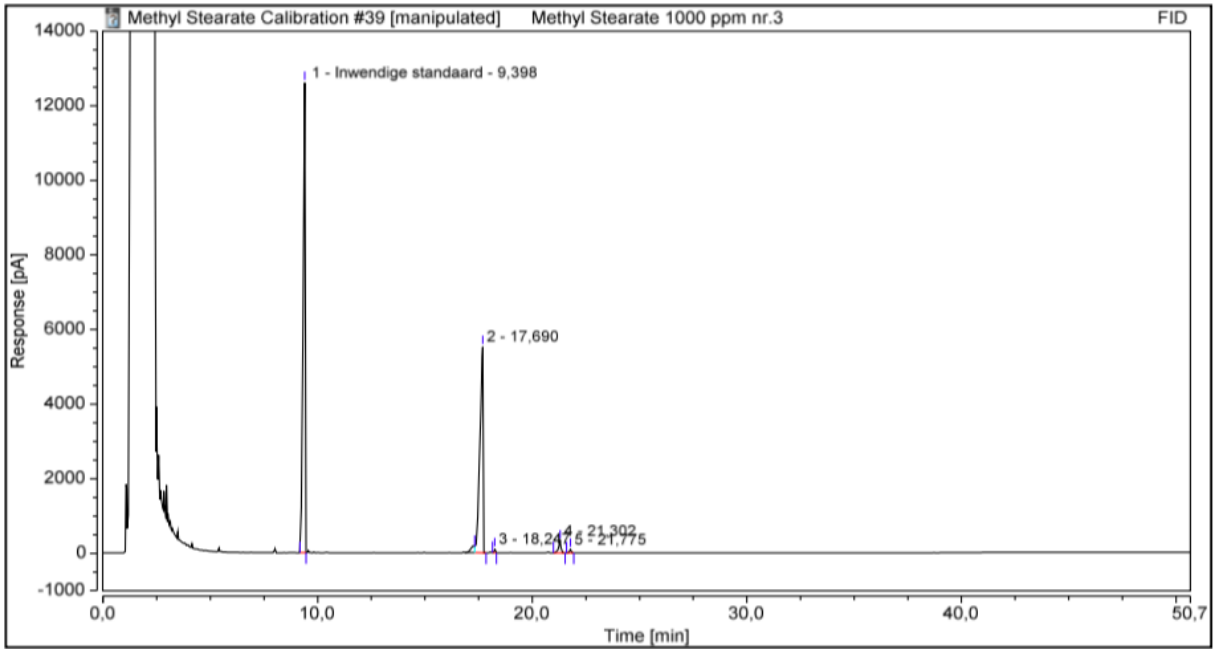

Methyl stearate 1000 ppm chromatogram.

.

Appendix 6. Palmitic Acid chromatograms signal

ppm	1st injection		2nd injection		3rd injection		Concentration	
	Area IS	Area Std	Area IS	Area Std	Area IS	Area Std	IS in vial (g)	Std in vial (g)
2.5	1153.071	0.426	1200.67	0.517	1184.657	0.561	0.001136	0.0000024381
5	1115.948	2.323	968.132	1.546	1027.975	1.868	0.001042	0.0000056852
10	1126.503	3.149	1079.388	2.684	986.758	2.578	0.001070	1.06409E-05
25	1185.666	9.835	1150.649	9.561	1200.142	10.505	0.001139	2.48261E-05
50	1210.9	23.228	1204.534	23.935	1179.442	24.628	0.001162	5.1102E-05
100	1134.721	54.62	1071.306	48.445	1017.769	45.13	0.001088	0.000102525
250	1145.678	127.646	1167.161	145.713	1085.569	126.528	0.001107	0.000247798
500	1063.436	292.522	1069.725	318.165	1040.139	295.082	0.001028	0.000524733
1000	817.423	528.287	827.247	532.42	826.59	551.002	0.001016	0.001015757

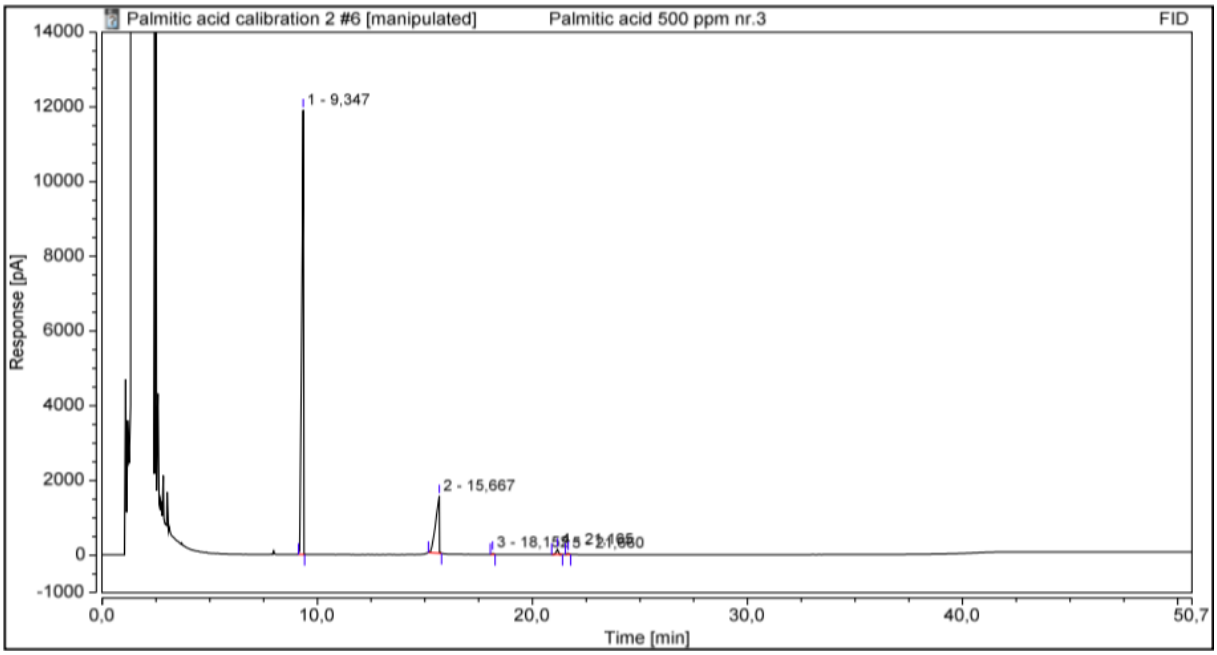

Palmitic acid 500 ppm chromatogram.

Appendix 7. Linoleic Acid chromatograms signals

ppm	1st injection		2nd injection		3rd injection		Concentration	
	Area IS	Area Std	Area IS	Area Std	Area IS	Area Std	IS in vial (g)	Std in vial (g)
1	1015.753	0	1013.045	0	987.962	0	0.001015	0.0000010839
2.5	445.334	0.438	981.301	0.158	1002.668	0.229	0.001028	0.0000026624
5	75.673	0.074	946.466	1.263	973.499	0.5	0.000822	0.0000057210
10	352.607	0	1012.364	2.079	988.296	1.561	0.000861	1.11176E-05
25	868.219	7.255	911.861	7.44	987.892	8.796	0.000808	2.70124E-05
50	1005.998	20.172	1044.621	21.929	1007.764	20.476	0.000841	5.48916E-05
100	1012.622	38.639	1026.296	37.368	1074.018	39.893	0.000830	0.000108932
250	987.089	96.173	1048.099	106.779	1021.098	109.292	0.000845	0.000263967
500	1029.904	235.742	1069.707	258.888	1087.447	249.919	0.000846	0.000547647
1000	769.246	461.761	799.298	472.984	813.414	510.001	0.001030	0.001096393

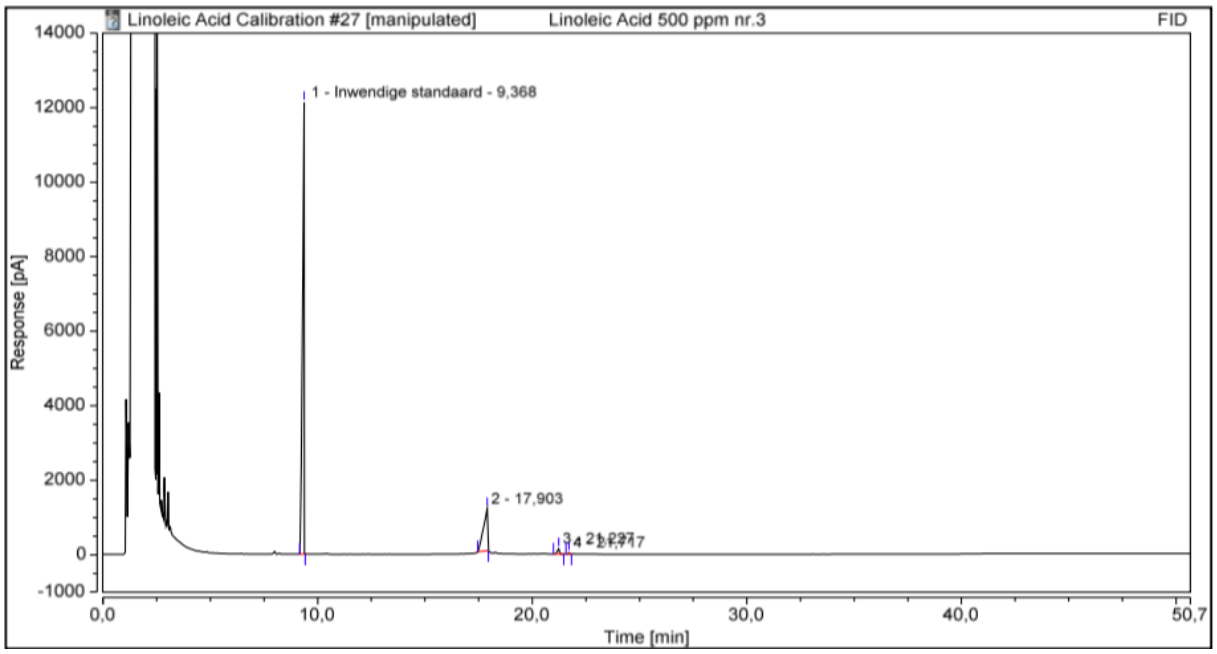

Linoleic acid 500 ppm chromatogram.

Appendix 8. Oleic Acid chromatograms signals

ppm	1st injection		2nd injection		3rd injection		Concentration	
	Area IS	Area Std	Area IS	Area Std	Area IS	Area Std	IS in vial (g)	Std in vial (g)
2.5	966.264	0.252	969.79	0.225	1006.646	0.24	0.001002	0.0000023056
5	150.529	0.16	840.071	0.509	856.644	0.461	0.001011	0.0000047786
10	713.879	1.173	459.85	0.583	1003.96	2.301	0.001154	9.08478E-06
25	94.828	0.353	929.93	7.709	983.293	8.346	0.001123	2.29376E-05
50	867.91	18.862	923.209	21.725	975.839	22.402	0.001096	4.77677E-05
100	860.54	47.979	819.784	44.516	812.174	46.222	0.001070	9.40225E-05
250	959.174	128.889	939.735	127.69	998.69	133.608	0.001110	0.000235149
500	920.797	292.672	978.499	305.367	998.887	320.314	0.001100	0.000497402
1000	915.33	560.008	935.985	603.33	932.749	542.9	0.001062	0.000954486

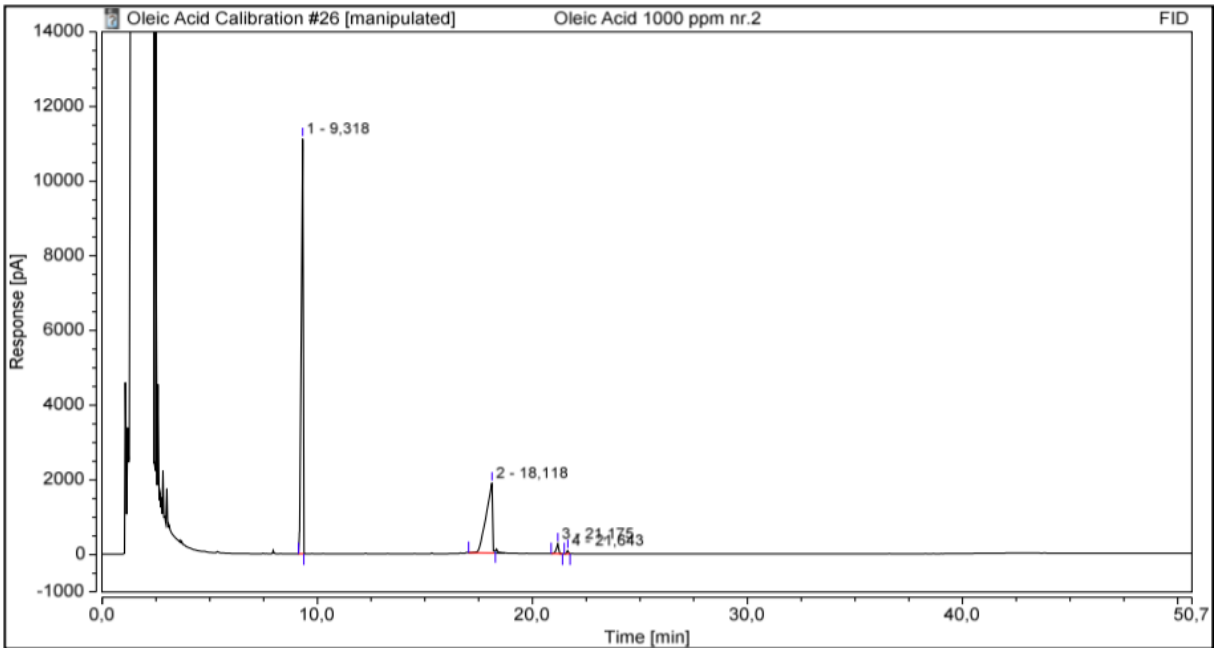

Oleic acid 1000 ppm chromatogram.

Appendix 9. Stearic Acid chromatograms signals

ppm	1st injection		2nd injection		3rd injection		Concentration	
	Area IS	Area Std	Area IS	Area Std	Area IS	Area Std	IS in vial (g)	Std in vial (g)
2.5	278.81	0	1022.795	0	1017.656	0	0.00097309	2.47251E-06
5	929.824	0.545	913.19	0.313	867.276	0.262	0.001047	0.000005
10	1024.476	1.69	973.395	1.761	1021.273	2.327	0.001128	0.000010
25	74.445	0.413	1010.116	6.931	965.924	6.617	0.001118	0.000026
50	296.222	2.513	942.008	18.146	985.46	19.247	0.001087	0.000052
100	937.075	36.615	944.204	43.814	1043.916	50.914	0.001093	0.000102
250	1000.165	119.898	990.715	118.465	1045.942	122.519	0.001146	0.000249
500	973.397	293.737	993.154	311.202	1015.371	319.593	0.001094	0.000520
1000	923.355	501.041	967.671	557.397	1024.588	612.323	0.001109	0.000985

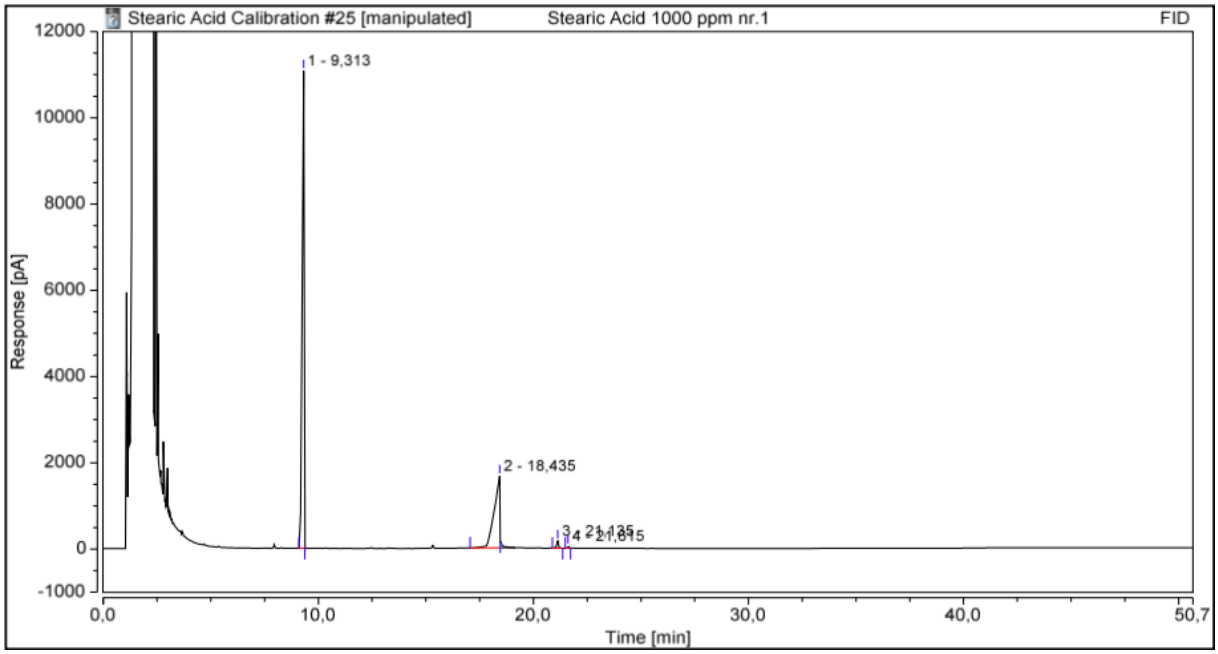

Stearic acid 1000 ppm chromatogram.

Appendix 10. α-tocopherol chromatograms signals

ppm	1st injection		2nd injection		3rd injection		Concentration	
	Area IS	Area Std	Area IS	Area Std	Area IS	Area Std	IS in vial (g)	Std in vial (g)
2.5	1230.677	0.969	1226.371	0.963	1214.807	1.112	0.000984	0.000003
5	1229.480	3.549	1221.109	3.197	1305.568	6.815	0.000893	0.000005
10	1343.857	6.476	1331.584	7.249	1340.739	7.346	0.001027	1.07417E-05
25	1214.056	23.639	1208.722	23.873	1213.489	25.105	0.000934	2.97575E-05
50	1274.246	45.254	1273.837	46.480	1277.177	45.798	0.001006	5.4225E-05
100	1463.842	94.967	1465.583	95.914	1461.182	95.284	0.001155	0.00010117
250	1294.369	259.628	1289.042	255.559	1296.861	257.145	0.000937	0.000264367
500	1289.661	478.822	1288.369	486.953	1289.125	482.349	0.001014	0.00052306
1000	1380.445	940.758	1373.946	917.994	1382.156	944.380	0.001073	0.000998773
2500	1312.603	2418.317	1308.672	2437.969	1314.585	2464.434	0.001054	0.002458583

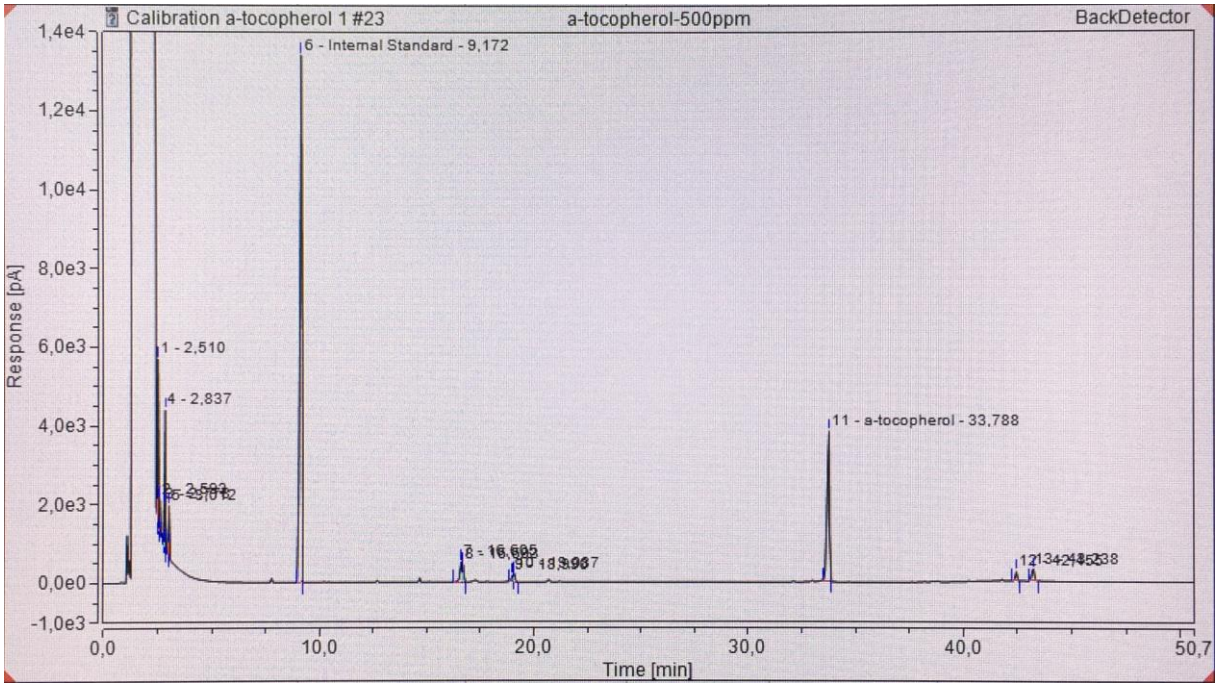

α-tocopherol 500 ppm chromatogram.

Appendix 11. DL-α-palmitin chromatograms signals

ppm	1st injection		2nd injection		3rd injection		Concentration	
	Area IS	Area Std	Area IS	Area Std	Area IS	Area Std	IS in vial (g)	Std in vial (g)
25	1279.634	8.114	1281.934	7.488	1282.457	7.776	0.000898	2.79121E-05
50	1418.900	18.554	1414.974	18.667	1413.129	18.194	0.001002	5.0466E-05
100	1427.829	42.828	1441.819	44.116	1427.068	42.860	0.001018	9.81397E-05
250	1415.765	119.429	1409.221	117.901	1406.684	117.788	0.001016	0.000232044
500	1384.473	308.992	1384.116	303.218	1396.340	306.638	0.000936	0.000532144
1000	1423.621	536.179	1420.631	520.523	1437.866	527.164	0.000993	0.000968901
2500	1496.150	1498.620	1492.880	1499.392	1502.368	1567.881	0.000974	0.002402145

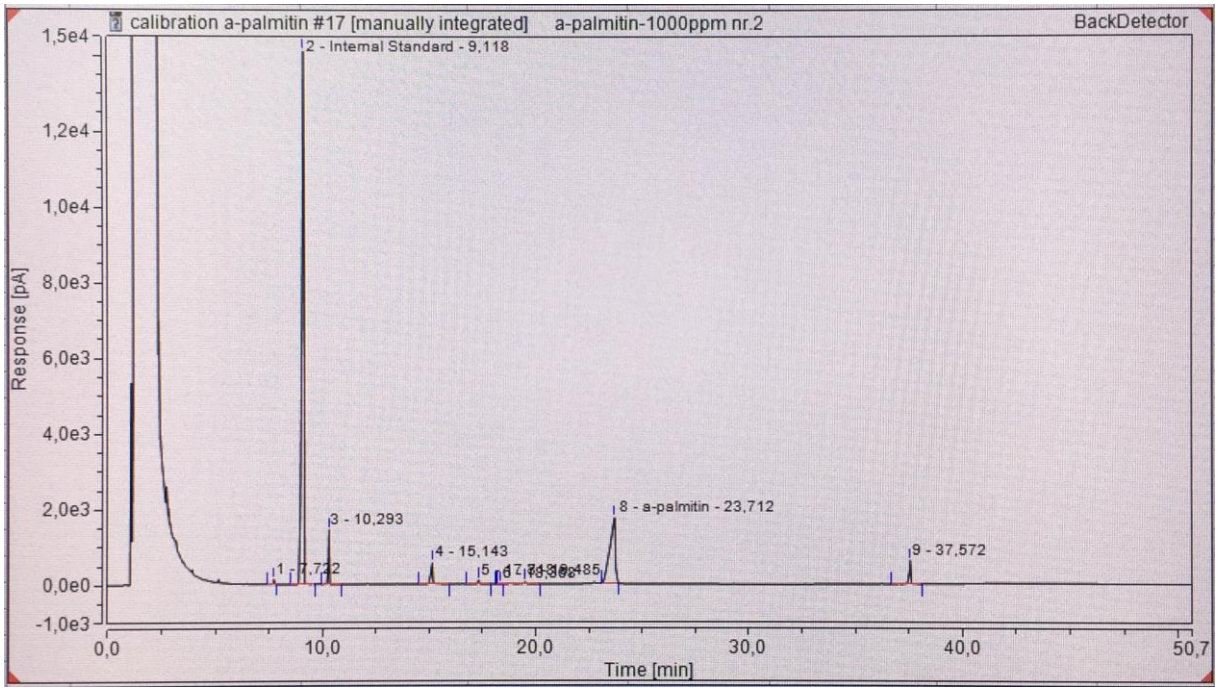

DL-α-palmitin 1000 ppm chromatogram.

Appendix 12. Tricaprylin chromatograms signals

ppm	1st injection		2nd injection		3rd injection		Concentration	
	Area IS	Area Std	Area IS	Area Std	Area IS	Area Std	IS in vial (g)	Std in vial (g)
0.5	1460.912	0.723	1453.451	0.745	1454.977	0.757	0.001063	0.000001
1	1390.381	1.265	1390.504	1.236	1393.369	1.287	0.001000	0.000001
2	1443.872	2.033	1447.247	2.034	1443.460	2.061	0.001034	2.01403E-06
5	1444.917	4.860	1442.863	4.835	1446.149	4.914	0.001030	5.13139E-06
10	1467.654	8.895	1469.748	9.016	1465.059	9.091	0.001036	9.75697E-06
20	1469.713	18.705	1484.180	19.185	1488.784	19.319	0.001034	2.207E-05
50	1556.717	40.343	1553.961	40.863	1561.027	41.808	0.001086	5.01042E-05
100	1520.709	82.141	1529.245	84.025	1527.005	82.462	0.001058	0.000104099
200	1467.455	152.141	1467.124	154.971	1457.790	151.046	0.001037	0.000198992
500	1442.969	375.398	1448.041	389.075	1453.313	381.020	0.001020	0.000489547

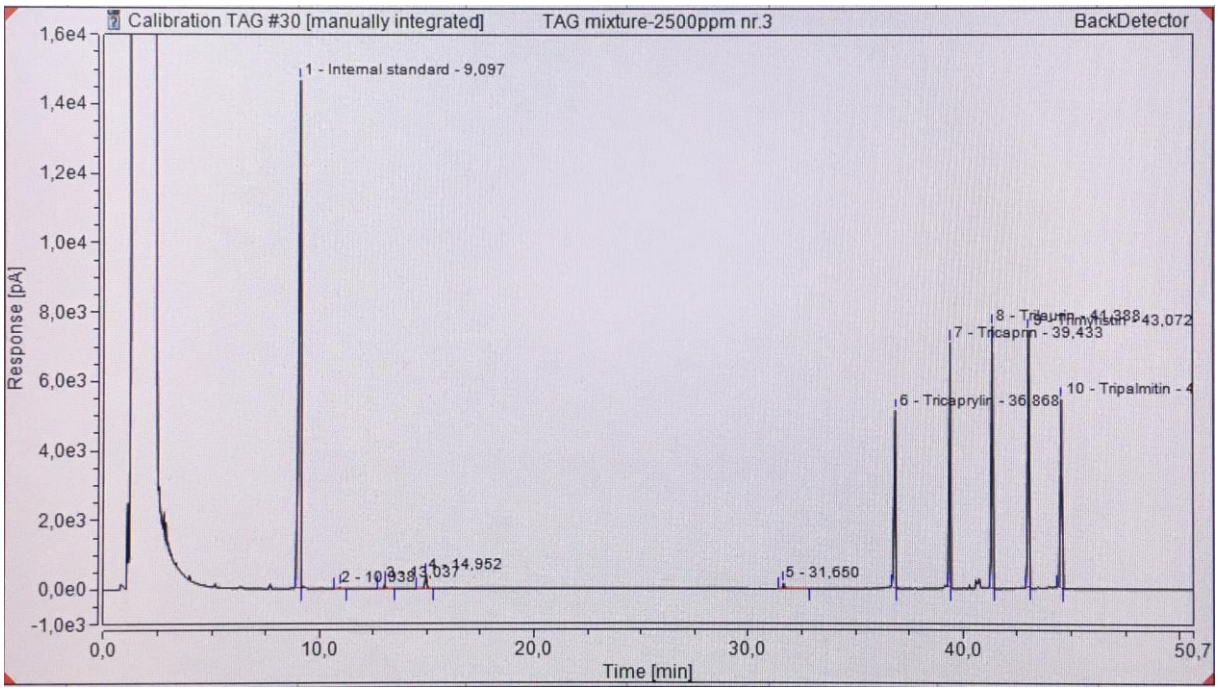

TAGs mixture 2500 ppm chromatogram.

Appendix 13. Tricaprin chromatograms signals

ppm	1st injection		2nd injection		3rd injection		Concentration	
	Area IS	Area Std	Area IS	Area Std	Area IS	Area Std	IS in vial (g)	Std in vial (g)
0.5	1460.912	0.630	1453.451	0.743	1454.977	0.743	0.001063	0.000001
1	1390.381	0.039	1390.504	1.223	1393.369	1.289	0.001000	0.000001
2	1443.872	2.081	1447.247	2.086	1443.460	2.068	0.001034	2.01605E-06
5	1444.917	4.950	1442.863	4.863	1446.149	4.858	0.001030	5.13653E-06
10	1467.654	8.978	1469.748	9.201	1465.059	9.274	0.001036	9.76674E-06
20	1469.713	20.108	1484.180	20.821	1488.784	20.544	0.001034	2.20921E-05
50	1556.717	46.352	1553.961	46.140	1561.027	26.999	0.001086	5.01543E-05
100	1520.709	95.632	1529.245	97.112	1527.005	97.153	0.001058	0.000104203
200	1467.455	189.199	1467.124	184.663	1457.790	182.351	0.001037	0.000199191
500	1442.969	445.556	1448.041	446.787	1453.313	381.020	0.001020	0.000490038

Appendix 14. Trilaurin chromatograms signals

ppm	1st injection		2nd injection		3rd injection		Concentration	
	Area IS	Area Std	Area IS	Area Std	Area IS	Area Std	IS in vial (g)	Std in vial (g)
0.5	1460.912	0.211	1453.451	0.390	1454.977	0.446	0.001063	0.000001
1	1390.381	0.540	1390.504	0.872	1393.369	0.870	0.001000	0.000001
2	1443.872	1.391	1447.247	1.484	1443.460	1.423	0.001034	2.01605E-06
5	1444.917	4.405	1442.863	4.406	1446.149	4.400	0.001030	5.13653E-06
10	1467.654	8.755	1469.748	8.883	1465.059	9.036	0.001036	9.76674E-06
20	1469.713	20.382	1484.180	20.871	1488.784	20.919	0.001034	2.20921E-05
50	1556.717	47.837	1553.961	49.132	1561.027	49.764	0.001086	5.01543E-05
100	1520.709	104.039	1529.245	105.545	1527.005	106.074	0.001058	0.000104203
200	1467.455	201.054	1467.124	202.282	1457.790	199.523	0.001037	0.000199191
500	1442.969	488.940	1448.041	485.168	1453.313	489.312	0.001020	0.000490038

Appendix 15. Trimyristin chromatograms signals

ppm	1st injection		2nd injection		3rd injection		Concentration	
	Area IS	Area Std	Area IS	Area Std	Area IS	Area Std	IS in vial (g)	Std in vial (g)
2	1443.872	0.375	1447.247	0.435	1443.460	0.352	0.001034	2.01605E-06
5	1444.917	1.926	1442.863	2.159	1446.149	2.192	0.001030	5.13653E-06
10	1467.654	5.358	1469.748	5.543	1465.059	5.637	0.001036	9.76674E-06
20	1469.713	16.585	1484.180	17.440	1488.784	17.323	0.001034	2.20921E-05
50	1556.717	43.050	1553.961	45.003	1561.027	45.876	0.001086	5.01543E-05
100	1520.709	100.443	1529.245	103.029	1527.005	103.235	0.001058	0.000104203
200	1467.455	195.940	1467.124	198.514	1457.790	196.927	0.001037	0.000199191
500	1442.969	485.175	1448.041	481.970	1453.313	484.672	0.001020	0.000490038

Appendix 16. Tripalmitin chromatograms signals

ppm	1st injection		2nd injection		3rd injection		Concentration	
	Area IS	Area Std	Area IS	Area Std	Area IS	Area Std	IS in vial (g)	Std in vial (g)
5	1444.917	1.528	1442.863	1.739	1446.149	1.446	0.001030	5.13139E-06
10	1467.654	2.487	1469.748	2.477	1465.059	2.308	0.001036	9.75697E-06
20	1469.713	6.028	1484.180	7.311	1488.784	7.097	0.001034	2.207E-05
50	1556.717	22.502	1553.961	25.001	1561.027	26.999	0.001086	5.01042E-05
100	1520.709	65.795	1529.245	70.043	1527.005	70.816	0.001058	0.000104099
200	1467.455	142.558	1467.124	145.380	1457.790	145.169	0.001037	0.000198992
500	1442.969	377.035	1448.041	382.411	1453.313	383.626	0.001020	0.000489547